Analysis of Petroleum Coke Consumption in Some Industrial Sectors

Aldo Ramos Santos*[1], Rogério José da Silva[2], Maria Luiza Grillo Renó[2]

[1]Dept. of Chemical Engineering, Universidade Santa Cecília, Av. Oswaldo Cruz 266, Santos-SP, Brazil

[2]Institute of Mechanical Engineering, Universidade Federal de Itajubá, Av. BPS 1303, Itajubá-MG, Brazil

*[1]rsantos@unisanta.br; [2]rogeriojs@unifei.edu.br; [2]malureno@yahoo.com.br

Abstract

The world production of petroleum coke has been growing in the last years, due to a growing supply of heavy oils. The market is divided among the green coke consumers and the calcinate coke consumers. When taking pollutants into consideration, the quality of petcoke depends on the type of processed petroleum and the operational conditions of the production unit. Three different processes can produce petcoke. The cost of petcoke is inversely proportional to its sulfur content. Due to the consumer process type, there are those who can only use coke with low sulfur content. However, there are consumers that can burn coke with larger sulfur content without needing exhausted gas desulfurization treatments, such as power plants with fluidized bed boilers, and in the cement industry where the sulfurous gases incorporate to the clinker in the form of calcium sulfate.

Keywords

Petroleum Processing; Petcoke; Desulfurization; Power Plants; Cement Industry

Introduction

Petroleum coke is a byproduct of the oil refining industry. It has a high calorific value and a low cost. Due to higher amounts of processed heavy oils, petroleum coke production has been increasing. Its low cost and abundance has made it an attractive residue for the industrial sector, especially for the electric power and cement production sectors (Wang et al, 2004). As oils become heavier, their densities in API degrees decrease and their contaminant content, especially sulfur compounds, may increase. This tendency becomes evident as presented in the data in Figure 1, part of a survey done on about 15.5 million barrels of oil processed per day in the U.S., of which two-thirds are currently imported from various parts of the world (EIA, 2012).

Due to the demand for petroleum with lighter production fractions such as naphtha, gasoline, kerosene and diesel, oil refineries have begun processing heavier oils to meet the market demand for light and medium products. Thus, along with the fluid catalytic cracking, which converts diesel into gases and gasoline, delayed coking has been increasing and gaining more and more importance in refineries (ANP, 2003). Since petroleum coke is a product derived from the bottom of the barrel oil processing system, this derivative has more or less sulfur content based on the type of oil from which it originated. Therefore cokes can have high and low sulfur content (Salvador et al, 2003; Barros et al, 2003). The high sulfur is a great problem because the sulfur emission control becomes the challenging. In literature there are many technologies for SO_2 emission control , as example using CaO sorbent or thermal desulfurization process (Wang et al, 2004).

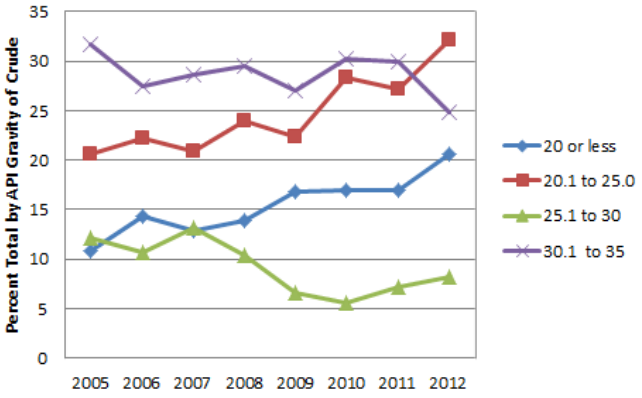

FIGURE 1. PERCENTAGE EVOLUTION OF IMPORTED CRUDE OIL, BY API GRAVITY BY USA, OF 2005 TO 2012 (EIA, 2012).

Types of Production Processes of Petroleum Coke

According to Speight (2004), coke production can be achieved by three different processes: delayed coking, coking in a fluidized bed and coking in a fluidized bed with gasification. Since coke originates from heavier petroleum fractions, it is natural that its denser impurities become concentrated, like metals and sulfur compounds; the content of these components depends

2168-5517/15/01 001-07, © 2015 DEStech Publications, Inc.
doi: 10.12783/jpsr.2015.0401.01

directly on the quality of the processed oil. Therefore, there can be cokes in the international market with sulfur contents ranging from about 4.0 to 7.5% by mass (Salvador et al, 2003). The coke produced in Brazil has sulfur contents averaging between 0.7 and 0.8 % by mass (Barros et al, 2003).

Comparative Composition of Coke Produced

All three of the production processes of petroleum coke have different process and operational configurations, which have a direct effect on the composition of the coke produced by each one of the three processes mentioned above (Speight, 2004). Table 1 shows the composition of the coke produced by the three processes, using traditional loads of vacuum residue, but originated from different oils. The table only shows the H/C relation to the condition of the process, since the loads do not have the same origin.

TABLE 1. COMPARISON BETWEEN THE PETROLEUM COKE PROCESS.

Composition (% in mass)	PetroleumCoke–ProductionProcess		
	Delayed	Fluidized Bed	Fluidized Bed with Gasification
C	87.9(1)	86.3	94.9
H	3.51(1)	2.2	0.3
H / C	0.47(1)	0.31	0.04
N	1.61(1)	2.4	1.1
S	7.5(1)	6.9	2.8
O	-	0.9	0
Ashes	0.33(1)	1.3	1.0
d (g / cm³)	2.00(2)	0.80	0.96

Source: Adapted of Furimsky (2000), Salvador et al.(2003)(1) and Garcia (2002)(2).

World Production of Petroleum Coke

The world production of petroleum coke reached 81 Mt (million tons) in 2001, 83 Mt in 2002 and was expected to surpass 88 Mt in 2005 (Dynamis, 2004). The United States of America is the largest producer of petroleum coke, accounting for about 66% of the world production. About 57% of the American production comes from the Gulf of Mexico (Texas and Louisiana). In the United States, about 35 refineries produce petroleum coke in considerable quantities (over 1000 t/day). Table 2 shows world production of coke, with the percentage share by region (Dynamis, 2004). Countries that export petcoke, according to Petcoke Report - April - 2007 (Energy Publishing, 2007) are presented in Table 3 and shows the absolute supremacy of the U.S. as a producer and exporter of petroleum coke

The total market value of petroleum coke was around 100 million tons in 2011 (Roskill, 2012). The United States accounted for 40% of the supply, while China produced 24 million tons. The market is bound by the demands of five major industries: petroleum refining, electric power generation, cement, steel and aluminum. The aluminum and steel industries require coke with higher purity, low sulfur and low levels of metals, especially in the aluminum industry for the production of high quality electrodes.

TABLE 2. WORLD PRODUCTION OF PETROLEUM COKE.

Regions Producers	Participation (%)
North America	69.5
South America	9.1
Europe	8.5
Asia	6.9
Ex-URSS	5.0
Africa	0.5
Oceania	0.5

Source: Dynamics (2004).

Price of the Petroleum Coke

Several factors influence the petroleum coke market price. When the international price of coal increases, the demand for petroleum coke also increases. According to analysts, the rise of the international coal price is generally what most influences the high price of the petroleum coke, usually with a delay of about 3 months. Figure 2 presents the evolution, in US$/million of BTU, of the petroleum coke price in relation to the cost of natural and synthetic gases produced by petroleum coke gasification (GCPA, 2005).

TABLE 3. EXPORTING COUNTRIES OF PETROLEUM COKE IN JANUARY AND FEBRUARY 2007.

Country	January - 2007				February - 2007			
	PetroleumCoke(t)				Petroleum Coke (t)			
	Green	Calcined	Total	%	Green	Calcined	Total	%
Canada	12052	6577	18629	0.66	8155	5347	13507	0.65
China	77815	55006	132821	4.71	80519	51078	131597	6.28
United Kingdom	20035	17899	37934	1.35	4932	24564	29496	1.41
United States	2383861	245021	2628882	93.28	1619898	299736	1919634	91.7
Total (jan/2007)			2818266		Total (fev/2007)		2094234	

Source: Energy Publishing (2007).

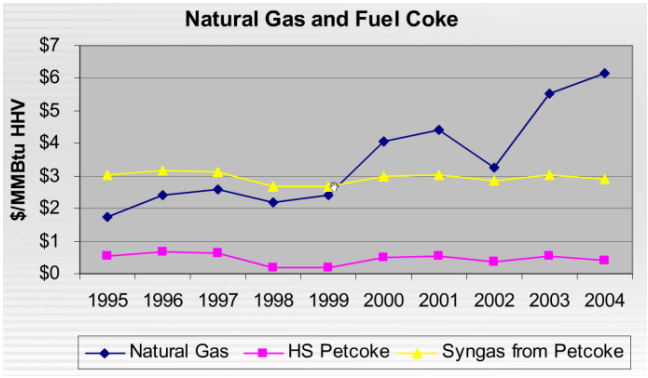

FIGURE 2. EVOLUTION OF THE PRICE OF PETROLEUM COKE, GAS NATURAL AND SYNTHETIC GAS DERIVED FROM PETROLEUM COKE (GCPA, 2005).

Table 4 shows a price comparison (relative to December 2012) between the cokes produced in the gulf region of the U.S. and in Venezuela. It shows that sulfur content interferes more with the prices than the HGI - Hardgrove Index. With the exception of the coke produced in the West Coast of the U.S., there was a price uptrend (Energy Publishing, 2012). The price stability of petroleum coke in recent years has also been an incentive for its use. Figure 3 shows a price comparison (March of 2007) between the petcoke produced in the U.S. gulf region and in Venezuela (Energy Publishing, 2007).

TABLE 4. PRICES OF PETROLEUM COKE IN FUNCTION AND SULPHUR CONTENT OF HARDNESS HGI.

Origin	Shulphur (%)	HGI	Price (US$/t)
United States (Gulf region) and Venezuela	4 – 5	<50	62.00 a 68.00
	6	35 a 45	50.00 a 56.00
	6	50 a 70	51.00 a 57.00
United States (West Coast)	3	45 a 50	80.00 a 87.00
	4+	45 a 50	73.00 a 79.00

Source: Energy Publishing (2012).

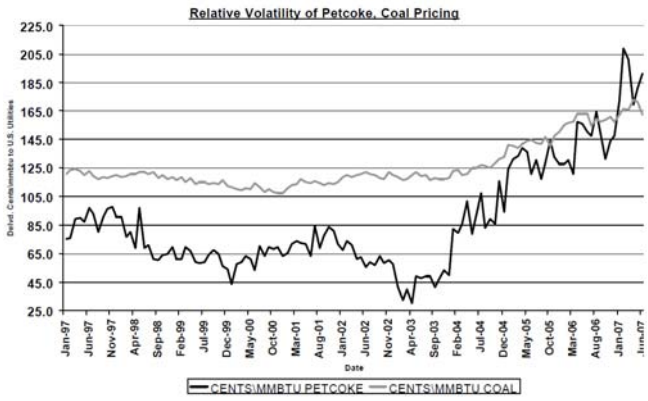

FIGURE 3. VOLATILITY ON BETWEEN THE PRICES OF COAL AND PETROLEUM COKE.
Source: Energy Publishing (2007).

Figure 3 shows that petroleum coke price was always below coal. However, from July of 2004, the increase of petroleum coke prices led them increasingly close to that of coal. In July of 2006 and January of 2007, petroleum coke prices surpassed the price of coal. On the other hand, the amount of petroleum coke which a refinery produces has little or nothing to do with the market value. In fact, refineries do not decide to produce more petroleum coke when the market demand increases and prices rise.

The sole reason for the production of petroleum coke growth is when greater amounts of heavy petroleum fractions are converted into lighter fractions such as in aviation fuel and gasoline, which create more residues. However, if a refinery is producing more heavy fractions, such as fuel oil, the process produces less petroleum coke.

Green Petroleum Coke (GPC) and Calcined Petroleum Coke (CPC)

The coke obtained directly from the delayed coking process is called green coke due to the greater volatile content in its composition. In another unit of operation, green coke is subjected to a calcination process, forming the so-called calcined coke, whose volatile content is greatly reduced. In the green coke calcination process, the sensible and latent heat of the volatile matter are recovered in a heat recovery boiler, which generates steam in a suitable pressure level for use in other units in the plant or sold to nearby green coke calcinations plants. Therefore, the production of steam can be considered an indirect consumable product obtained in the petroleum coke production. Table 5 shows the comparative composition between the green coke and the calcined coke by anode grade. This Table shows the great difference between the volatile matter content contained in green coke and calcined coke. Table 5 also shows that calcined coke HGI is smaller than that of the green coke HGI. As the HGI is inversely proportional to the coke's grindability, it shows that green coke is more suitable for used as fuel when compared to the calcined coke, because less energy is used in the grinding process.

The global market of calcined coke is a highly competitive one with participants from various countries. Petroleum coke is used as fuel in India, China, Japan, Russia, Germany, the U.K., France, the U.S., Canada, Venezuela, Mexico, Argentina and Brazil. (Martinez and Bartholomew, 1998 apud Ellis and Paul, 2000; Globaldata, 2012).

In 2009, Brazil imported about 3.75 million tons of petroleum coke and produced 3.5 million tons. The

steel industry consumed about 825,000 tons. However, the largest consumer of petroleum coke was the cement industry. Currently in Brazil, the only green petroleum coke calcinator is Petrocoque S.A., located in the city Cubatão, in the São Paulo State, in an area close to the PresidenteBernardes Refinery. Petrocoque receives the green coke from PresidenteBernardes Refinery of Cubatão, a Petrobras unit, and via a calcination process, in which the rotary kiln operates at 1.8 rpm and 1300 °C, produces the calcined coke, whose main application is the manufacture of electrodes for aluminum metallurgy (Lind, 2003).

TABLE 5. COMPOSITION CHARACTERISTIC OF GREEN AND CALCINED COKE (ANODE).

Composition	Green Coke	Calcined Coke (anode)
Volatile Matter (%)	9.0 ~ 10.5	0.08 ~ 0.15
Moisture (%)(1)	8.0 ~ 14	0.2 ~ 0.4
Ashes (%)	0.09 ~ 0.14	0.10 ~ 0.18
Sulphur (%)	0.70 ~ 0.85	0.70 ~ 0.78
Vanadium (ppm)	180 ~ 230	200 ~ 250
Nickel (ppm)	180 ~ 200	200 ~ 220
Silicon (ppm)	40 ~ 80	20 ~ 60
Iron (ppm)	80 ~ 120	60 ~ 100
Sodium (ppm)	70 ~ 90	50 ~ 100
Calcium (ppm)	20 ~ 40	20 ~ 40
Hardgrove Index (HGI) (1)	70 ~ 80	20 ~ 40

Source: PETROCOQUE (2003) and Hammond et al.(2003)(1).

Processes that Uses Petroleum Coke

Depending on the supply to the consumer market, there are cases where the calcined coke is used as fuel in thermoelectric power plants and cement plants with high volatile content (12%t) and the high value of HGI (100). Other advantage is that the calcined petroleum coke has a high energy content compared to mineral coal and low ash content (typically 0.1 wt%).

The thermoelectric power plant usually use coal with low sulfur content mixed with petroleum coke with high sulfur content, with aim to emit SO_2 in acceptable values for the environmental legislation.

The work of Olmeda et al. (2012) introduces a new way to use petroleum coke as lightweight aggregate in cement mortars to make sound barriers. The acoustic behaviour herein was assessed by constructing a large dimension mortar slab (made of cement and coke as aggregate) used as floor covering and measuring. Results showed that coke addition leads to a decrease in mechanical properties of resultant mortars, this is principally due to an increase of the porosity (60%). A gradual increase of impact noise insulation was observed in light weight floor covering from middle to higher frequencies tested, reaching, within this range, a remarkable improvement of sound insulation compared to control slab (14 dB).

The green coke may have the following uses (Ellis and Paul, 1998): fuel coke used in cement production and in fluidized bed boilers to generate steam and electrical energy, using limestone to remove sulfur compounds; if it presents low-sulfur content, the petroleum coke may have metallurgical use in the form of mixtures composed with mineral coke, for blast furnace feed; undergoing partial oxidation, the petroleum coke can be used in gasification processes for applications in water steam production in electric power generation; and in the production of gas for various industrial applications. The green coke can also be used directly in the blast furnace, in a process known as injection of coal fines. In this process the green coke, also used as fuel, is blended with other coals, pulverized and injected directly into the blast furnaces.

Other applications,suchassupplementing metallurgical coalusedin coke batteriesforsteel productionorthe direct use inthe production of siliconcarbide, alsoprovide highvaluemarketsfor green coke (Garbarino, 2007). Table 6 presents a summary of the uses of green coke.

TABLE 6. APPLICATTIONS TO GREEN PETROLEUM COKE.

Applications of the Green Coke	Markets	Required Quality
Raw material for calcination	Aluminum TiO_2	Low volatile (Max. 12%) Low levels of metals Lowsulfur (<2%)
Carbon-basedreducer	Pig Iron Iron Alloys Carbides	Low sulfur (< 1.0%) High fixed carbon (>90%) Low levels of metals Granulometry (iron alloys and pig iron)
Raw material for coke kiln	Foundry	Low sulfur (<1.0%) High fix carbon (>90%)
Raw material for coke kiln	Greatsteel industries	Low sulfur (<1.0%) High fix carbon (>90%)
Fuel	Lime Great steel industries Ceramic red Pelletizing/Sintering	Low sulfur (<10%) High calorific value
Fuel	Cement Kiln Power Plants	High sulfur (>4%) High calorif value

Source: Carvalho and Assis(2007).

In Brazil, the larger demand for calcined petroleum coke occurs in the aluminum industry that uses it to produce carbon anodes. Its purpose is to conduct electric current in orderto obtain an electrolytic reaction of alumina dissociation for the production of primary aluminum (Silva et al, 2009).

Beside this application, other industrial application is the titanium production from titanium oxide and calcine petroleum coke. The main process steps are chlorination, reduction and electrolysis igneous, this technology is called Kroll process (Zahner, 1995). Table 7 shows the worldwide consumption of calcined coke.

TABLE 7. WORLDWIDE CONSUMPTION OF CALCINED COKE.

Industrial Segment	Consumption of petroleum coke (tons)
Aluminum Industry	9,880,000
Steel Industry	1,040,000
Re-carburizing market	910,000
Titanium dioxide	650,000
Industry others	520,000

Source: Dickie, 2006.

These applications are being used successfully in Brazil, in COSIPA – CompanhiaSiderúrgicaPaulista in Cubatão, SP, making the steel sector yet another consumer of petroleum coke (BR-N° 20, 2005).

Figure 4 shows the electrical energy production in the U.S. in 2009, based on the type of fuel used, showing that the thermoelectric plants contributed with 50.1% of the total production, presenting itself as a potential consumer of petroleum coke (FCEL, 2005; EIA, 2012). The World Energy Council recommends that the mixture of mineral coal and petroleum coke contain at most 20% of coke, due to the low content of volatile material in the petroleum coke (WEC, 2005).

New Technologies for Consumption of Petroleum Coke

According to Furimsky (1999), the supply of heavy oils has increased in the world market. Processing these oils has generated less light products and more heavy residues. Thus, there will be a tendency for refineries to use residue from gasification processes in refineries of origin, producing gas streams, which may serve as raw materials for other processes.

Edison International and British Petroleum had planned on developing a 1 billion dollar power plant in an oil refinery located in California. The plant would produce 500 MW using the byproduct of the petroleum coke gasification, with operation expected in 2011 (Reuters, 2006).

Wang et al (2004) proposed a process having zero SO_2 and CO_2 emissions with an expected application for petroleum gasification. The coke is burned in a fluidized bed, using CaO for absorbing SO_2 and CO_2. A calciner, burning coke, may be used to regenerate the CaO and obtain CO_2 for other industrial processes. The loss of CaO will be due to its conversion into $CaSO_4$, forcing the replacement of $CaCO_3$ through the calciner.

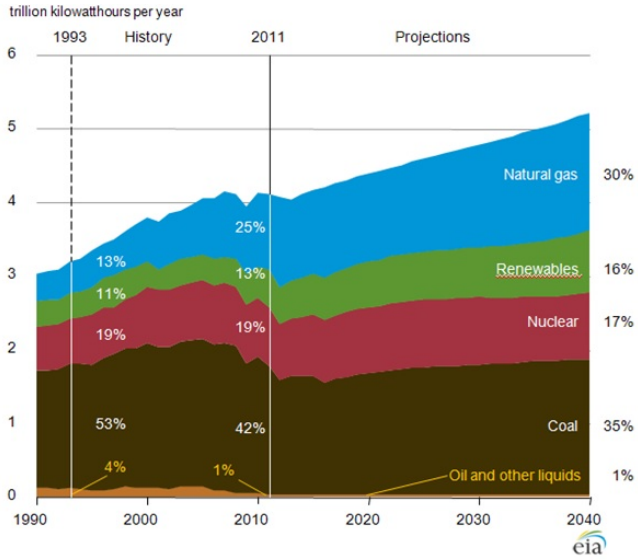

FIGURE 4. ELECTRIC POWER GENERATION IN THE UNITED STATES, IN 2010 (EIA, 2012).

Environmental Legislation

Due to sulfur contents, normally present in much of the petroleum coke available in the international market, among the parameters controlled by the Environmental Legislation, this study is primarily concerned with the emission limits of SO_2, due to the fact that this pollutant is produced by burning petroleum coke.

In the U.S., the emissions standard for SO_2 established by EPA for kilns of cement clinker production depends on the location, atmospheric dispersion conditions and proximity to population centers. In the European Union, the established standards vary from country to country, but they are measured under the conditions of 25 °C, 101.3 kPa and 11% O_2 corrected, in the exhausted gases, in dry basis. Under these conditions, it is considered that, for emissions below to 1000 mg SO_2/Nm^3, it is recommended gases be treated by using limestone and, for emissions slightly over 1000 mg SO_2/Nm^3, systems of dry or moist scrubbers are used. For the kilns of clinker production it is recommended to keep emissions between 170 and 340 mg SO_2/Nm^3 (PA, 2005).

In Brazil, CONAMA Resolution Nº 5 of 06/15/89, according to the Revision on September 19th, 2005 limited emissions nationally by typology of sources of priority pollutants. The CONAMA Resolution No 8 of 12/06/90, which is in a revision process, establishes

that for fixed sources with power less than 70 MW the emissions limit is 5,000 g SO_2/Mkcal (coal or fuel oil). For fixed sources with power greater than 70 MW, the emissions limit is 2,000 g SO_2/Mkcal (coal or fuel oil). The CONAMA Resolution Nº 382 of 12/26/2006 establishes the maximum emission limits for air pollutants from fixed sources. In Article 7, paragraph 1, it cites that the Environmental Agency may establish values less restrictive than the maximum emission limits established in this Resolution, considering the technological limitations and the impact in the local conditions according to the provisions of CONAMA Resolution Nº 5 of 06/15/89. Article 8 established that limits and criteria established by CONAMA Resolution Nº 8 of 12/06/90 for the processes of heat generation not covered by this Resolution should remain applicable. CONAMA Resolution N° 382 in ANNEX XI - Emission limits for air pollutants from Portland cement industry does not establish emission limit for sulfur oxides (SO_X), advocating on its item 7 that "according to the local characteristics of the area of influence of the polluting source to the air quality, the Environmental Agency may establish more restrictive emission limits, inclusively considering the alternative use of fuels with lower pollution potential". In the State of São Paulo, the emission standard for the cement industry is from 350 mg SO_2/Nm^3 to 7% O_2 corrected in exhausted gases, in dry base (Busato, 2004). In Paraná State, Brazil, Resolution N° 041/02 establishes emission limits of SO_2 for source generators of thermal potency, according to the Table 8 (SEMA-PR, 2002). For clinker production kilns, the same resolution establishes the limit of 400 mg SO_2/Nm^3, with 7% O_2 corrected in the exhausted gases in dry basis.

TABLE 8. EMISSION LIMITS FOR SO_2, TO 7% O_2 CORRECTED IN THE EXHAUST GASES IN DRY BASIS, AS RESOLUTION 041/02, STATE OF PARANÁ-BRAZIL.

Thermal Power (MW)	mg SO_2/Nm^3
< 10	-
10 – 50	3,000
50 – 100	1,400
> 100	400

Source: SEMA – PR (2002).

Conclusions

The increase of petroleum coke production is a natural consequence of the increase of oil API degree, currently available in the international market. This trend is reflected in the discovery of large non-conventional oil reservoirs, extremely heavy and with high sulfur content. Thus, the current consumer market of petroleum coke must be amplified, whether by encouraging current customers to increase their quotas, or including new technologies for the use of petroleum coke. It must also be taken into account the possibility of coal blends with low sulfur content, aiming to reach the important consumer market of thermoelectric power plants. Therefore, there is a balance between the production and the consumption of this residue of oil processing. However, whichever route is to be taken for the use of the petroleum coke, the consumers must comply with the emission standards for pollutants, especially in relation to the SO_2.

References

ANP - Agência Nacional de Petróleo. 2003. Available in http://www.anp.gov.br. Accessed in 2003.

BR-No 20 – Petrobras Distribuidora. N° 20, Ano 4, Julho/Agosto, 2005, BR. Available in http://www.br.com.br/Portalbr. Accessed in 2005.

Barros, F.et al. Coking Considerations, Hydrocarbon Engineering. June, pp. 61-65, 2003.

Busato, L., C. VI FIMAI. Seminário de Co-Processamento. Formação e controle de emissões em fornos de produção de cimento. 2004.(in Portuguese)

Carvalho, R. L. and Assis, P.C.L. Coque Verde de Petróleo: Uma visão geral sobre qualidade, produção no Brasil e exterior e suas aplicações. PETROBRAS S.A., 2007. Available in http://www.petrobras.com.br/minisite/premiotecnologia/pdf/carbono2007.pdf (in Portuguese). Accessed in 2007.

CMS – Cement Manufacturing Sector. Foundation Report on the Cement Manufacturing Sector. 2004.

CONAMA – Conselho Nacional do Meio Ambiente - Brasil. Resolução CONAMA 8, de 06/12/1990. Available in http://www.mma.gov.br. Accessed in 2005.

CONAMA – Conselho Nacional do Meio Ambiente - Brasil Resolução CONAMA 382, de 26/12/2006. Available http://www.mma.gov.br. (in Portuguese). Accessed in 2007.

CONAMA – Conselho Nacional do Meio Ambiente – Brasil. Resolution CONAMA 5, de 15/06/1989, Revised in 19/09/2005. Available in:http://www.mma.gov.br/port/conama/res/res89/res0589. (in Portuguese). Accessed in 2005.

Dickie, R. Calcining growth and expansion.8° Carbon

Conference – Greats Lakes Carbon, Houston, 2006.

Dynamis – Coque de Petróleo: Parte 1; Parte 2; Parte 3.Available www.dynamismecanica.com.br/industrias. htm. (in Portuguese) Accessed in 2004.

EIA – Energy Information Administration/Petroleum Marketing Monthly December. 2012.

Ellis, P. J. and Paul, C.A. Tutorial: Delayed Coking Fundamentals. Great Lakes Carbon Corporation.1998.

Ellis, P. J. and Paul, C. A. Tutorial: Petroleum Coke Calcining And Use of Calcined Petroleum Coke. Great Lakes Carbon Corpotarion. 2000.

Energy Publishing, LLC Domestic and International. Petcoke Report. March. 2007.

Energy Publishing, LLC Domestic and International. Petcoke Report. March. 2012.

FCEL – FuelCell Energy Inc. Available in http://www.fce. com/downloads/wabash.pdf. Accessed in 2005.

Fisher, P. H. A competitive advantage for buyers and sellers of petroleum coke. Petcoke Consulting LLC. Available in: petcokeconsulting.com. Accessed in 2013.

Furimsky E. Gasification in Petroleum Refinery of 21st Century. Oil & Gas Science and Technology. 1999.

Furimsky, E. Characterization of cokes from Fluid/flexi-coking of heavy feeds. FuelProcessing Technology. 2000.

Garbarino, R. M. The outlook for green coke used in aluminum smelting 2007 - 2011. CRU Aluminum Conference. 2007.

Garcia, R. Combustíveis e combustão industrial. Editora Interciência. Rio de Janeiro. 2002. (in Portuguese)

GCPA – Gulf Coast Power Association, 14 April 2005, ConocoPhillips, Petroleum Coke Gasification Synergies for Refineries.

Globaldata.Petroleum Coke Industry to 2015. Available in: http://www.globaldata.com. Accessed in 2012.

Hammond, D., G. et al. Review of fluid bed coking technologies. ExxonMobil Research and Engineering Company.PTQ AUTUMN 2003. Available in: http://www.prod.exxonmobil.com/refiningtechnologies/ pdf/Autumn03PTQFLKArticlepdfforweb.pdf. Accessed in 2005.

IEA-COAL – IEA Clean Coal Center. United Kingdom. Available in: http://www.iea-coal.org.uk/content//default. asp?PageId=604&LanguageId=0. Accessedin 2004.

Lind, M. Petroleum Coke - Petrocoque S.A. Personal information to the author. Cubatão. 2003.

Olmeda, J. et al. Recycling petroleum coke in blended cement mortar to produce lightweight material for impact noise reduction. Cement & Concrete Composites 34. pp 1194 – 1201. 2012.

PA – Power Alstom. Coal Fired Power Plant.Availablein: http://www.power.alstom.com/power-generation-equipment/coal-fired-power-plant.htm.Accessed in 2005.

PETROCOQUE – Petrocoque S.A. Laboratório de Controle de Qualidade. Cubatão. SP. 2003.

Reuters. Edison International, BP plan $ 1 bln power plant: report.Available in www.reuters.com. Accessed in 2006.

Roskill. Petroleum Coke: Global Industry Markets & Outlook. 6th Edition. 2012. Available in http:// www.roskill.com. Accessed in 2012.

Salvador, S. et al. Reaction rates for the oxidation of hightysulphurized petroleum cokes: the influence of thermogravimetric conditions and some coke properties. Fuel 82.2003.

SEMA-PR – Secretaria de Meio Ambiente do Estado do Paraná-Brazil. 2004.

Silva, E. P. et al. Empiric mathematical models for real density of calcined coke based on industrial data. 2009. Availablein http://www. myalacd.com. Accessed in 2013.

Speight, J., G. New Approaches to Hydroprocessing. Catalysis Today. Vol 98, Issues 1-2, 24 November, pp. 55-60. 2004.

Swain, E. J. Petroleum coke production from US refineries will increase. Oil & Gas Journal/Nov. 2003.

United Nations. Petroleum Coke. UNdata – A world of Information. United Nations Statistics Division. (data.un.org) 2013.

Wang, J. et al. Clean and efficient use of petroleum coke for combustion and power generation. Fuel 83. 2004.

WEC – World Energy Council. Challenges and Economics of Using Petroleum Coke for Power Generation. 2005. Available in http://www.worldenergy.org. Accessed in 2005.

Zahner, L. W. Architectural Metals. John Wiley and Sons 1995. Available in http://www.books.google.com. Accessed in 2013.

Comparative Study of the Characterization Factors for Hydrocarbon Types of Petroleum Fluids Fractions

Djamel El-Hadi

Laboratory of Functional Analyses of Chemistry Process, Engineering Process Department, Blida 1 University, Soumâa B.P 270 Blida, 09000 (Algeria)

elhadidjamal@gmail.com

Abstract

The qualitative and quantitative determination of the chemical nature of the oil fractions is a very complex operation. For this reason, one often searches for empirical correlations, based on the introduction of different characterization factors. Considering the diversity of these factors, our study aims to establish a new criterion specific to the various factors. The application of three criteria (the separation order, the power separation and relative variation) has enabled us to determine the efficiency of each factor with respect to chemical nature of a petroleum fraction and to choose a certain number of factors, which can be used for the establishment of the various correlations. Thanks to these correlations we can determine the chemical composition, in paraffins, naphtenes and aromatics of petroleum fractions. The results obtained show that the characterization factors : CH (carbon to hydrogen weight ratio), (n/d) (refractive index to density ratio), Watson characterization factor (K) and that of El Hadi (F) can be applied to the characterization of light and heavy petroleum fractions.

Keywords

Characterization; Factor; Petroleum Fraction; Paraffin; Naphtene; Aromatic

Introduction

With an aim of characterizing the oil products from the chemical composition point of view, several empirical factors were proposed by various researchers. These factors are mathematical functions with one, two or three variables; and each variable represents a physical property such as: density, boiling point, index of refraction, molecular mass and viscosity. The importance of the use of these sizes is owing to the fact that practically all these last are additive properties for pure hydrocarbons. Put aside the carbon to hydrogen weight ratio CH, all the factors which we have just described, are empirical sizes, their determination is done indirectly. These factors can be introduced into correlations giving the physical properties or the chemical composition of the liquid oil fractions. Since the end of the 19th century, several empirical characteristic factors were proposed with an aim of determining chemical nature in such or such class. For the goal of justifying the utility of a given factor, we will make a rational comparative study, based on scientific criteria. The criteria proposed in this work are: separation order, power separation and relative variation.

Characterization Factors for Hydrocarbons

The realization of this study requires the calculation of the value of the factor (G) for three homologous series of hydrocarbons (API, 1978): n-alkanes (P), n-alkylcyclohexanes (N) and n-alkylbenzenes (A) at two different temperatures 80 and 200°C. For, we take into account the characterization factors which are a function of the physical properties: normal boiling point (Tb); density (d) at 20°C in g/cm^3; specific gravity (s) at 60/60°F; sodium D-line refractive index (n) at 20°C and 1 atm and molecular weight (M). The factors used for the realization of this study are : the specific refraction $R_1 = (n - 1) / d$ (Gladstone-Dale, 1863) or $R_2 = (n^2 - 1) / (n^2 + 2)\, d$ (Lorentz-Lorenz, 1880) ; the molecular refraction $R_{1M} = M\, R_1$ or $R_{2M} = M\, R_2$; Watson characterization factor $K = (Tb(°R))^{1/3}/s$ (Watson-Nelson, 1933) ; refractivity intercept $Ri = n - d / 2$ (Kurtz-Ward, 1936) ; correlation index $CI = (48640 / Tb(K)) + 473.7s - 456.8$ (Smith, 1940) ; the functions $G = M(d - 0.8513) / d + 23.6$ and $L = M(n - 1.4752) / n^2 + 4.51$ (Guilyazetdinov, 1959) ; characterization factor $I = (n^2 - 1) / (n^2 + 2)$ (Huang, 1977) ; the parameter $m = M (n - 1.4750)$ (Riazi-Daubert, 1986); characterization factor $F = (Tb(°R))^{1/3}/n^4$ (El Hadi, 2005) refractive index to density ratio n/d (El Hadi-Bezzina, 2005) ; and carbon

2168-5517/15/01 008-08, © 2015 DEStech Publications, Inc.
doi: 10.12783/jpsr.2015.0401.02

to hydrogen weight ratio CH. The latter is given by the formula of pure hydrocarbon $C_{ui}H_{wi}$: CH = 12ui / wi. To determine the capacity of separation of the existing factors, we associate of each factor by three criteria that are used as means of comparison.

Separation criteria

The Separation Order

At a given normal boiling point, the separation order is directly related to the nature of the physical property used; thus the density will increase according to the order: paraffins, naphtenes and aromatics ($d_P < d_N < d_A$). The refractive index has the same behaviour ($n_P < n_N < n_A$): while the molecular weight decreases in the same direction ($M_P > M_N > M_A$). We notice that the monotony is practically always satisfied, for all the physical properties (P→N→A or A→N→P). The results of table 1, show that the molecular refraction, defined by R_{1M} and R_{2M} is not able to separate the three hydrocarbons types and that the factors R_1, R_2 and Ri do not verify the monotony, already defined. On the other hand this property holds for the factors: K, CI, G, L, I, m, n/d, F and CH. The evolution of the various characterization factors of pure hydrocarbons according to the boiling point and of chemical nature is represented in figures 1.1-1.14.

Power Separation

The power separation (PS) is the most important characteristic, which quantitatively classifies all the factors satisfying the monotony. This criterion expresses the distance of paraffins or aromatic of the other two hydrocarbons types. If we manage to separate one of the hydrocarbons types in an effective way, the separation of both others does not pose any problem. The power separation in % is defined at a given temperature t (°C), by the two following formulas:

TABLE 1. VALUES OF CHARACTERIZATION FACTORS AT TEMPERATURES 80 AND 200 °C.

Factor (G)	P		N		A		Separation order
	$(G)_{80°C}$	$(G)_{200°C}$	$(G)_{80°C}$	$(G)_{200°C}$	$(G)_{80°C}$	$(G)_{200°C}$	
R_1	0.568	0.564	0.547	0.552	0.570	0.569	N < P < A
R_2	0.346	0.340	0.329	0.330	0.335	0.336	N < A < P
R_{1M}	52.01	89.79	45.88	83.90	44.53	82.32	–
R_{2M}	31.70	54.13	27.60	50.21	26.19	48.60	–
K	12.76	12.69	10.99	11.74	9.736	10.98	A < N < P
Ri	1.045	1.047	1.037	1.042	1.062	1.059	N < P < A
CI	0.168	-0.169	51.64	28.53	99.26	54.79	A > N > P
G	-1.391	0.129	15.68	14.45	26.06	24.88	A > N > P
L	-0.080	-0.005	2.470	2.177	5.408	5.366	A > N > P
I	0.232	0.252	0.256	0.265	0.295	0.288	A > N > P
m	-8.719	-9.048	-4.129	-4.829	2.039	1.924	A > N > P
n/d	2.063	1.911	1.833	1.797	1.708	1.733	A < N < P
F	2.372	2.343	2.081	2.185	1.693	1.929	A < N < P
CH	5.184	5.508	6.000	6.000	12.00	8.329	A > N > P

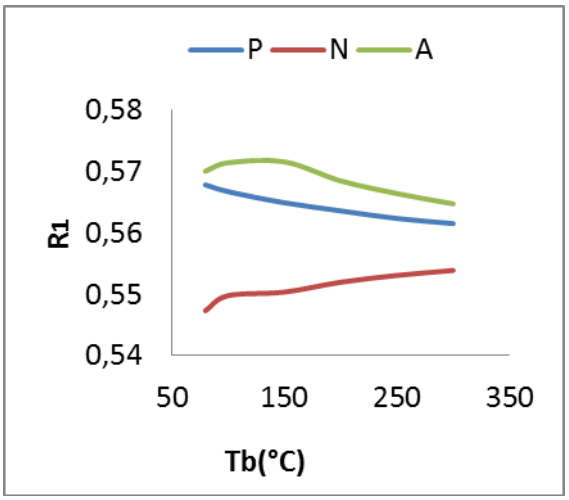

FIGURE 1.1. SPECIFIC REFRACTION (R_1).

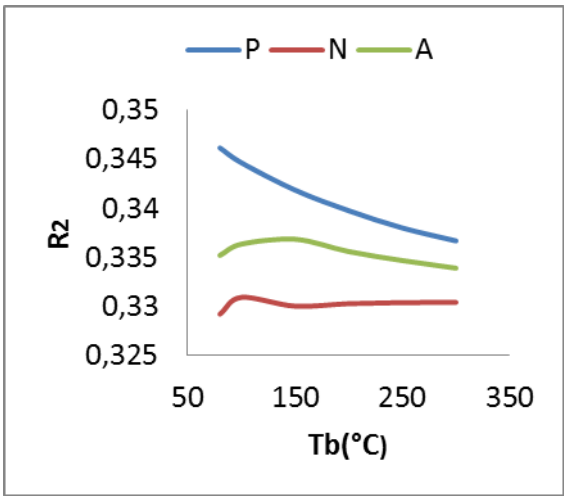

FIGURE 1.2. SPECIFIC REFRACTION (R_2).

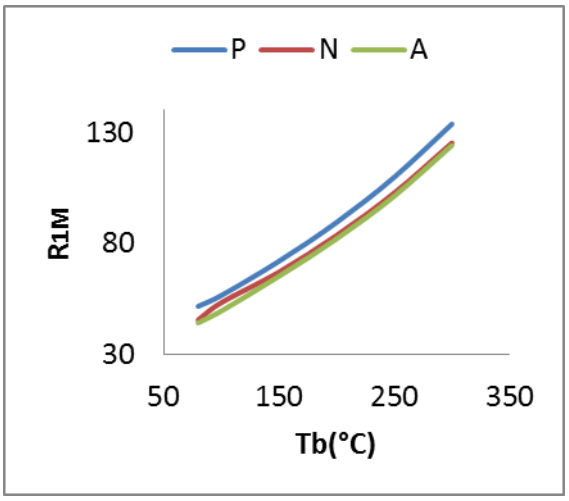

FIGURE 1.3. MOLECULAR REFRACTION (R_{1M}).

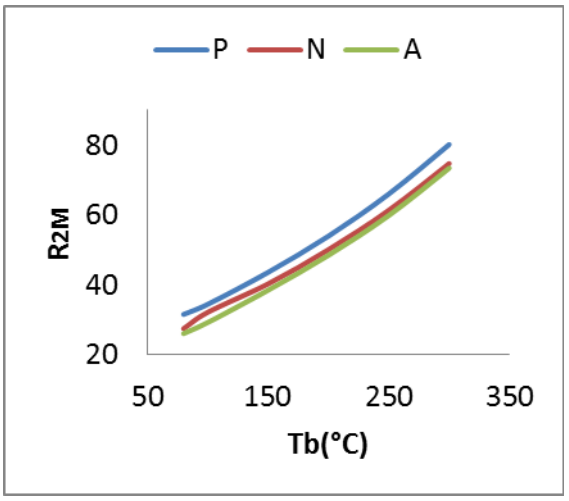

FIGURE 1.4. MOLECULAR REFRACTION (R_{2M}).

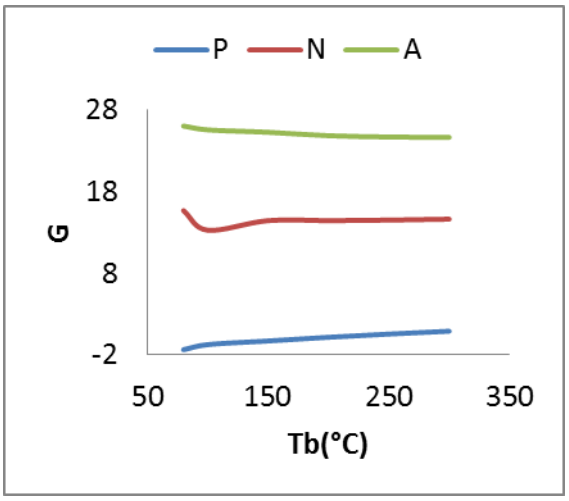

FIGURE 1.5. FUNCTION G OF GUILYAZETDINOV.

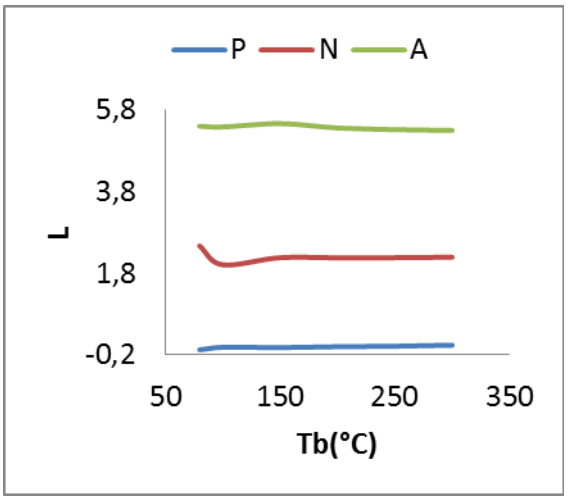

FIGURE 1.6. FUNCTION L OF GUILYAZETDINOV.

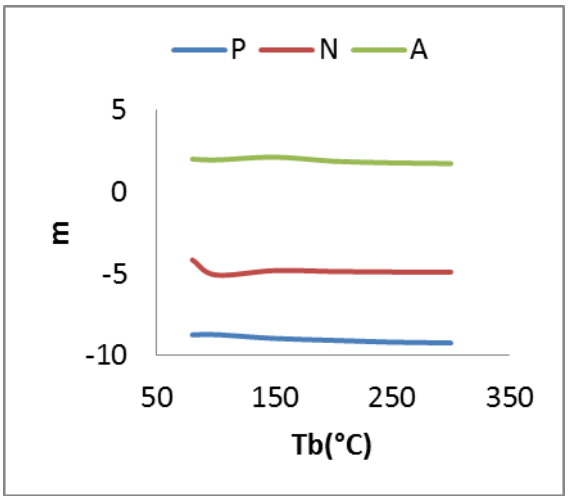

FIGURE 1.7. PARAMETER OF RIAZI-DAUBERT

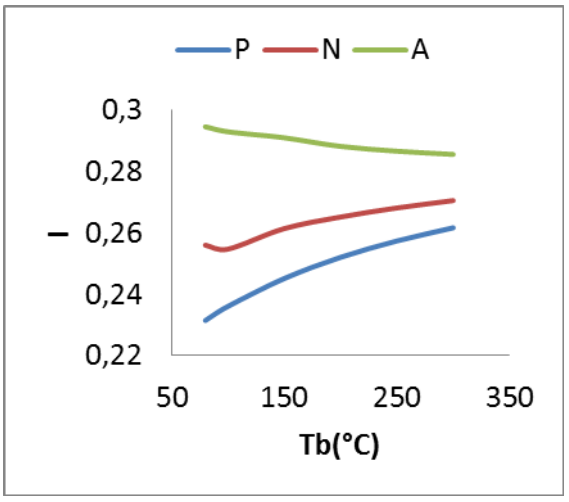

FIGURE 1.8. HUANG CHARACTERIZATION FACTOR.

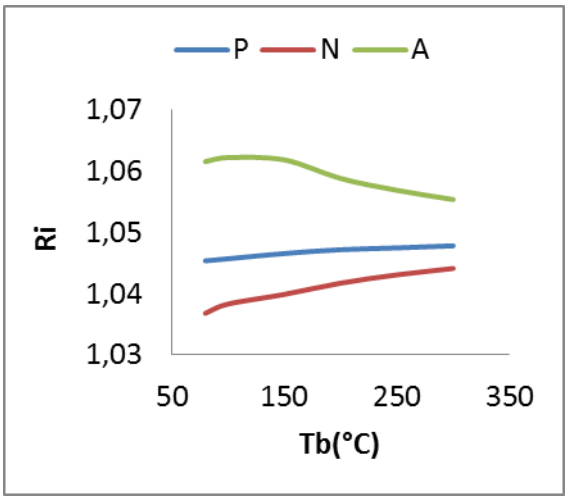

FIGURE 1.9. REFRACTIVITY INTERCEPT.

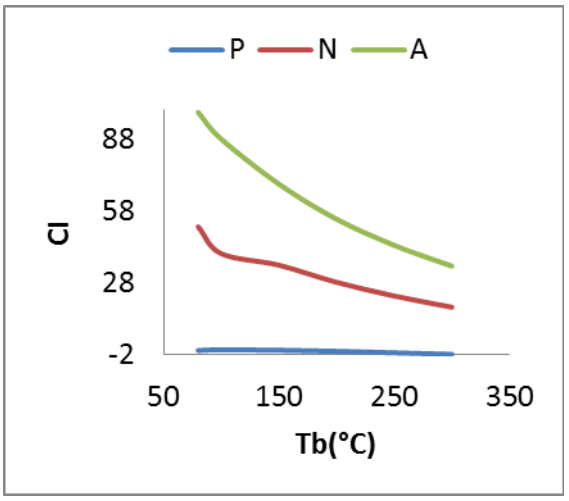

FIGURE 1.10. CORRELATION INDEX.

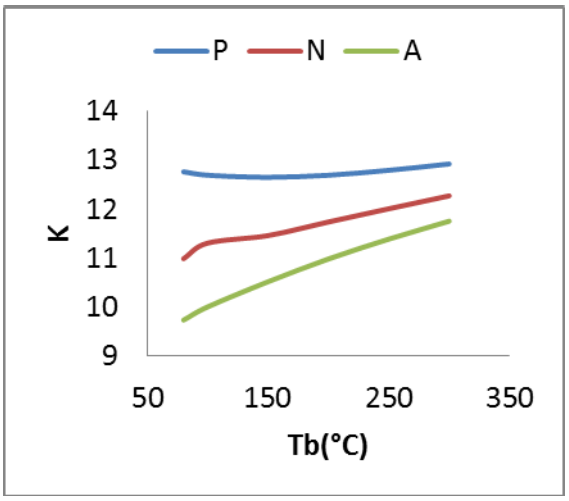

FIGURE 1.11. WATSON CHARACTERIZATION FACTOR.

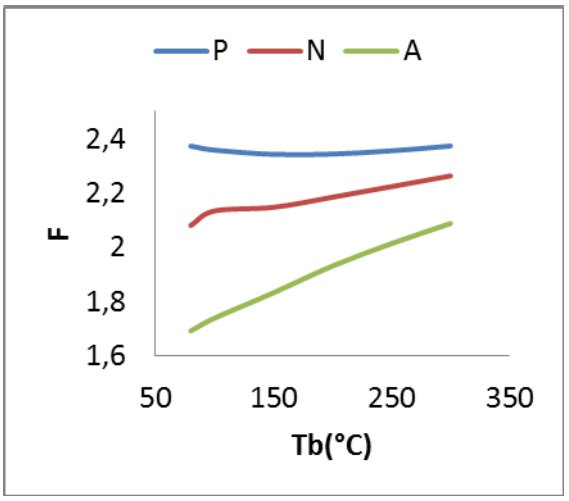

FIGURE 1.12. EL HADI CHARACTERIZATION FACTOR.

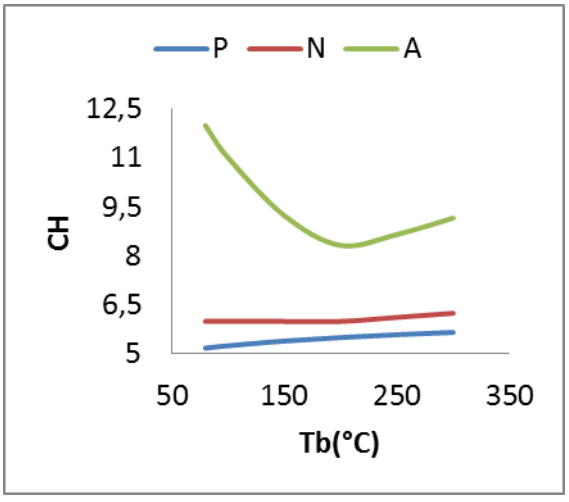

FIGURE 1.13. CARBON TO HYDROGEN WEIGHT RATIO.

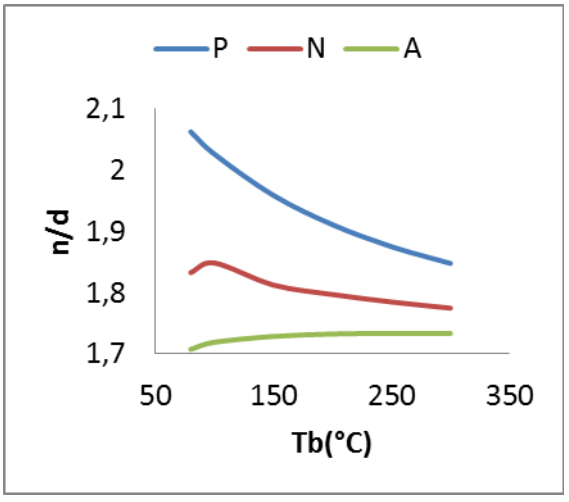

FIGURE 1.14. REFRACTIVE INDEX TO DENSITY RATIO.

TABLE 2. VALUES OF THE POWER SEPARATION AND THE RELATIVE VARIATION OF CHARACTERIZATION FACTORS.

Factor (G)	$(PS)_P$ in %			$(PS)_A$ in %			$(VR)_j$		
	80°C	200°C	$(PS)_{Pm}$	80°C	200°C	$(PS)_{Am}$	$(VR)_P$	$(VR)_N$	$(VR)_A$
K	58.53	55.56	57.05	41.47	44.44	42.95	0.02315	0.24800	0.41140
CI	51.94	52.22	52.08	48.06	47.78	47.92	0.00339	0.23240	0.44730
G	62.19	57.86	60.03	37.81	42.14	39.97	0.05539	0.04481	0.04299
L	46.47	40.62	43.54	53.53	59.38	56.46	0.01367	0.05345	0.00767
m	42.67	38.45	40.56	57.33	61.55	59.44	0.02967	0.06314	0.01037
I	38.92	36.19	37.56	61.08	63.81	62.44	0.32590	0.14400	0.10130
n/d	64.74	63.83	64.28	35.26	36.17	35.72	0.42680	0.10020	0.07062
F	42.86	38.16	40.51	57.14	61.84	59.49	0.04271	0.15317	0.34757
CH	11.97	17.44	14.70	88.03	82.56	85.30	0.04754	0.00000	0.53860

For paraffins:

$$(PS)_{P,t} = 100\ |(G)_{P,t} - (G)_{N,t}|\ /\ |(G)_{P,t} - (G)_{A,t}| \qquad (1)$$

For aromatics:

$$(PS)_{A,t} = 100\ |(G)_{A,t} - (G)_{N,t}|\ /\ |(G)_{P,t} - (G)_{A,t}| \qquad (2)$$

In our work, we calculate the (PS) at two temperatures: 80 and 200°C. The average power separation for the hydrocarbons type j ($(PS)_{jm}$) is given by the formula:

$$(PS)_{jm} = ((PS)_{j,80°C} + (PS)_{j,200°C}) / 2 \qquad (3)$$

A better separation of such a hydrocarbon type corresponds to a high value of (PS) of the used factor. The values of the power separation of the various factors are given in table 2. According to these results, we also can classify the various characterization factors by their descending orders of separation. Thus for paraffins, we have: n/d ($(PS)_{Pm}$ = 64.3%) > G ($(PS)_{Pm}$ = 60.0%) > K ($(PS)_{Pm}$ = 57.1%) > CI ($(PS)_{Pm}$ = 52.1%) and for the aromatics: CH ($(PS)_{Am}$ = 85.3%) > I ($(PS)_{Am}$ = 62.4%) > F ($(PS)_{Am}$ = 59.5%) > m ($(PS)_{Am}$ = 59.4%) > L ($(PS)_{Am}$ = 56.5%). In view of this classification, we immediately notice that the parameter (n/d) has the highest value of the power separation of paraffins ($(PS)_{Pm}$ = 64.3%); whereas for the aromatics, the carbon to hydrogen weight ratio (CH) is better ($(PS)_{Am}$ = 85.3%). These results confirm and justify our choice of the combination (CH, n/d) for the establishment of the correlations giving the composition of petroleum fractions (El Hadi-Bezzina, 2005). The CH factor characterizes the chemical structure of the molecules and separates better the aromatics from two other hydrocarbons types (P and N). On the other hand, the n/d ratio characterizes the physical behaviour of the molecules and separates paraffins from the other two hydrocarbons types (N and A).

The Relative Variation

In general all the characterization factors vary according to the boiling point. This variation expresses the stability of a factor on an a given temperature interval, for each studied class with respect to the total variation. The relative variation $(VR)_j$ is defined by the following formula:

$$(VR)_j = |(G)_{j,80°C} - (G)_{j,200°C}|\ /\ |(G)_{max} - (G)_{min}| \qquad (4)$$

The results given on the table 2, show that the majority of the characterization factors fix the paraffins; thus according to the relative variation values $(VR)_P$, these factors can be classified by their ascending orders of stability: CI ($(VR)_P$ = 0.0034) < L ($(VR)_P$ = 0.0137) < K ($(VR)_P$ = 0.0232) < m ($(VR)_P$ = 0.0297) < F ($(VR)_P$ = 0.04271) < CH ($(VR)_P$ = 0.0475) < G ($(VR)_P$ = 0.0554). The factors stabilizing the aromatics are classified according to their relative variations in the following ascending order: L ($(VR)_A$ = 0.0077) < m ($(VR)_A$ = 0.0104) < G ($(VR)_A$ = 0.0430) < n/d ($(VR)_A$ = 0.0706) < I ($(VR)_A$ = 0.101). Similarly for the naphtenes, these factors can be classified in the following order: CH ($(VR)_N$ = 0) < G ($(VR)_N$ = 0.0448) < L ($(VR)_N$ = 0.0535) < m ($(VR)_N$ = 0.0631) < n/d ($(VR)_N$ = 0.100). This study shows that in the considered temperature interval (80 - 200°C), the parameter CI ($(VR)_P$ = 0.0034) is the most stable for the paraffins, but its separation power is relatively weak: $(PS)_{Pm}$ = 52.1%. The same remark can be done for the parameter L with respect to the aromatics with a relative variation: $(VR)_A$ = 0.0077 and a separation power: $(PS)_{Am}$ = 56.5%. The carbon to hydrogen weight ratio CH is constant for the naphtenes, with a relative variation : $(VR)_N$ = 0.0000 and a relatively low paraffins variation: $(VR)_P$ = 0.0475; there fore this factor is most powerful for the separation of the aromatics: $(PS)_{Am}$ = 85.3%. We also notice that the factors K($(VR)_P$ = 0.0023) and F ($(VR)_P$ = 0.0042) are characterized by a weak relative variation with respect to the paraffins; thus the first separates the paraffins with an acceptable separation power: $(PS)_{Pm}$ = 57.1% and the second separates the aromatics

with a relatively high separation power: $(PS)_{Am}$ = 59.5%. The determination of these parameters has the advantage of using physical properties accessible by experiment (boiling point, density and refractive index) and a simple empirical formula.

Study of the Existence Plans

The use of the different combinations (G_1, G_2) for the qualitative or quantitative prediction of chemical nature of petroleum fractions, requires the study of the fields or the existence plans (G_2 = f (G_1)) of three hydrocarbons types. According to this representation (figure 2), we observe that the separation is perfect when the monotony of the two factors G_1 and G_2 is satisfied that is, for the same temperature interval, the factors used must separate the same class in the same order; eliminating any interference between the various classes by increasing the separation probability.

This characteristic is verified for the combinations represented in figure 2 (a) ((K, n/d), (K, F), (F, n/d)) ; figure 2 (b) ((CI, G), (CI, L), (CI, m), (CI, I), (CI, CH), (G, L), (G, m), (G, I), (G, CH), (L, m), (L, I), (L, CH), (m, I), (m, CH), (I, CH)) ; figure 2 (c) ((K, CI), (K, G), (K, L), (K, m), (K, I), (K, CH), (F, m), (F, I), (F, CH)) and figure 2 (d) ((CI, n/d), (G, n/d), (L, n/d), (m, n/d), (I, n/d), (CH, n/d), (m, F), (I, F), (CH, F)) ; therefore this type of combinations as it is shown on these figures will enable us to have a precise delimitation for each class. On the other hand the combinations represented in figure 2 (e) ((R_1, CI), (R_1, G), (R_1, L), (R_1, m), (R_1, I), (R_1, CH), (Ri, CI), (Ri, G), (Ri, L), (Ri, m), (Ri, I), (Ri, CH)) and figure 2 (f) ((R_2, K), (R_2, n/d), (R_2, F)) do not have this specificity, hence we can eliminate the

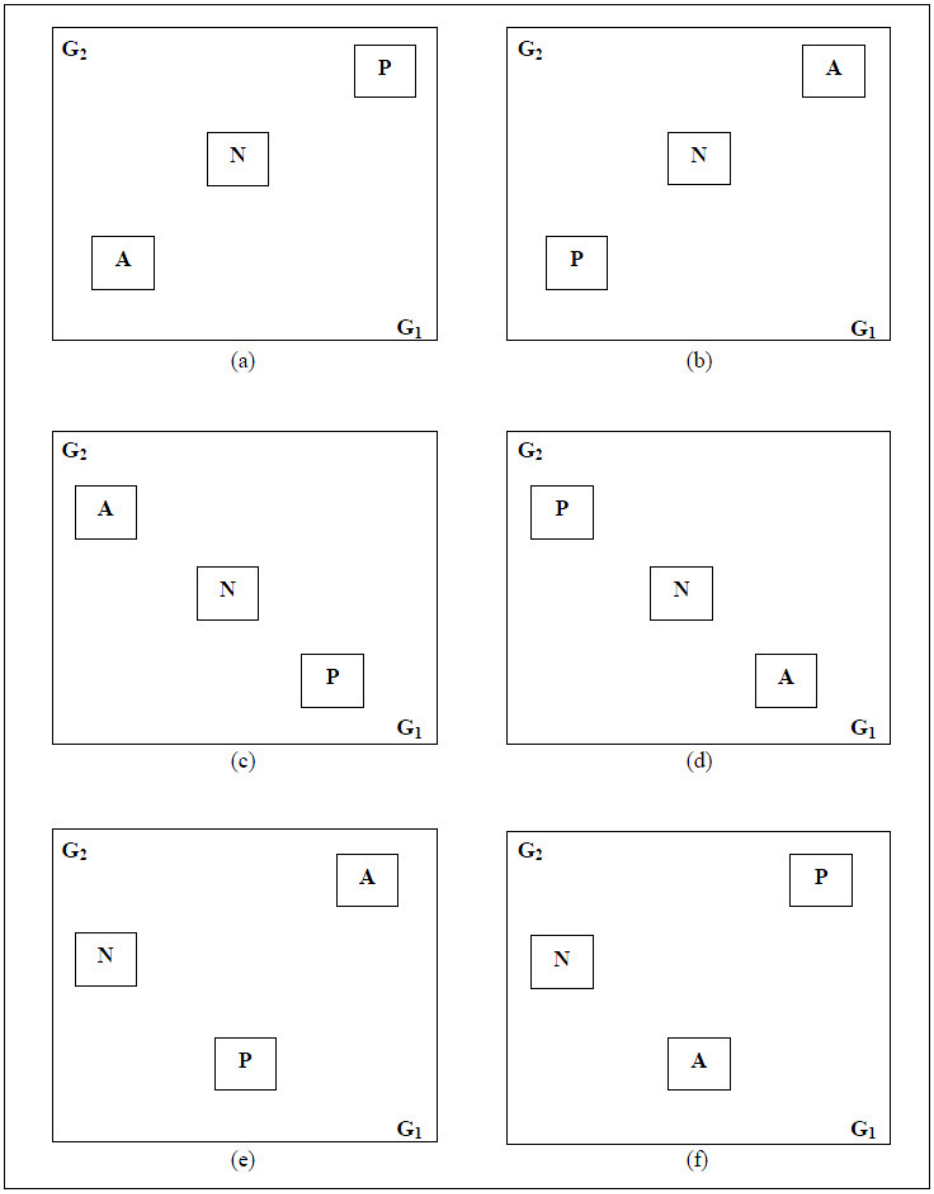

FIGURE 2. EXISTENCE PLANS OF THE THREE HYDROCARBON TYPES.

factors: R_1, R_2, R_{1M}, R_{2M} and Ri. Relying on this verification, we suggest that the factors having the same type of monotony can be combined with each other. The factors that do not verify the monotony (like the refractivity intercept (Ri)); can be used for the separation of the mixtures with two hydrocarbons types (Kurtz and al., 1958 and ; Nwadinigwe-Okoroji, 1990).

Conclusions

In view of this study, we claim that the effectiveness of such a characteristic factor depends on several criteria; thus the criterion already used qualitatively by various authors (Riazi-Daubert, 1986 and Vakili-Nezhaad, 2002) is the relative variation. The latter characterizes the stability of a characteristic factor on a given temperature interval for a hydrocarbon type studied with respect to the total variation of this factor. But it does not determine the distance from a hydrocarbon type with respect to the other. For this purpose, the proposal of the two other criteria has considerably contributed to the development of a correct classification of the various characteristic factors. This study shows that the power separation (PS) is the most powerful criterion, used to express the distance from a hydrocarbon type with respect to the others. During the application of the various combinations (G1, G2) to separate the three hydrocarbon types, we noticed that the separation order influences directly on the monotony of separation (P→N→A or A→N→P). For a given boiling point, the results obtained demonstrate that the factors n/d ($(PS)_{Pm}$ = 64.3% and $(VR)_A$ = 0.0706), CH ($(PS)_{Am}$ = 85.3% and $(VR)_N$ = 0.0000), K ($(PS)_{Pm}$ = 57.1% and $(VR)_P$ = 0.0232) and F($(PS)_{Am}$ = 59.5% et $(VR)_P$ = 0.04271) are very effective for the determination of the chemical nature of the petroleum fractions. The main results have led to the proposal of two new factors (F and n / d) and to the confirmation of the effectiveness of the two others (CH and K) . These factors are functions of the physical properties (average boiling point Tb, density d and refractive index n) which are accessible by the experiment with a high degree of accuracy. The factors L ($(VR)_P$ = 0.0137, $(VR)_A$ = 0.0077 and $(PS)_{Am}$ = 56.5%), G ($(VR)_N$ = 0.0448 and $(PS)_{Pm}$ = 60.0%) and m ($(VR)_A$ = 0.0104 and $(PS)_{Am}$ = 59.4%) are characterized by weak relative variations, but their separation powers are relatively weak compared to the factors n/d, CH, K and F. Moreover these factors depend on the molecular weight: a physical property of petroleum fractions which cannot be determined with precision. This study has also enabled us to choose the best combinations (G_1, G_2) for the quantitative prediction of the chemical composition in paraffins, naphtenes and aromatics of petroleum fractions. The best combinations are (n/d, CH) for narrow fractions and (K, F) for large fractions.

Nomenclature

A = Aromatic

°C = Celsius degree

CH = Carbon to hydrogen weight ratio

CI = Correlation index of Smith

d = Density at 20°C, in g/cm 3

F = El Hadi characterization factor

G, L = Functions of Guilyzetdinov

$(G)_{j,t}$ = Characterization factor of the classe j, measured at the temperature t (°C)

I = Huang characterization factor

K = Watson characterization factor

M = Molecular weight

m = Parameter of Riazi-Daubert

N = Naphtene

n = Sodium D-line refractive index at 20°C and 1 atm.

P = Paraffin

$(PS)_j$ = Power separation of the classe j (j = P, A)

R = Specific refraction

°R = Rankine degree

Ri = Refractivity intercept

R_M = Molecular refraction

s = specific gravity at 60/60

Tb = Normal boiling point

$(VR)_j$ = Relative variation of the classe j (j = P, N, A), in the interval (80 - 200°C)

REFERENCES

American Petroleum Institute (API) Research Project 44, "Selected Values of Properties of Hydrocarbons and Related Compounds." Tables of Physical and Thermodynamic Properties of Hydrocarbons, A and M Press, College Station, Texas, extant, 1978.

El-Hadi, D. "Simulation d'une distillation TBP par la caractérisation des fractions distillées en paraffines, naphtènes et aromatiques." Thèse de doctorat d'état en

génie des procédés, U. S. D. Blida, Algérie, Octobre 2005.

El-Hadi, D. and Bezzina, M. "Improved empirical correlation for petroleum fraction composition quantitative prediction." *Fuel*, 84, 611–617, 2005.

Gladstone, J. M. and Dale, T. P. "Researches on the dispersion, refraction and sensitivity of liquids." Trans. Roy. Soc. London, A 153, 317, 1863.

Guilyazetdinov, L. P. "A new method for Structural Analysis of hydrocarbon fuels and oils." Khim. Teknol. Topl. Masel, 8, 42–49, 1959.

Huang, P.K., Ph.D. Thesis, Department of Chemical Engineering, The Pennsylvania State University, University Park, Pa., 1977.

Kurtz, S. S., Jr. and Ward, A. L. "The refractivity intercept and the specific refraction equation of Newton I. Development of the refractivity intercept and comparioson with specific refraction equations." J. Franklin Inst., 222, 563–592, 1936.

Kurtz, S. S., Jr., King, R. W., Stout, W. J. and Peterkin, M. E. "Carbon–Type composition of viscous fractions of petroleum, Density–Refractivity intercept method." Anal. Chem., 30, 7, 1224–1236, 1958.

Lorentz, H. A., Wied. Ann., 9, 64, 1880.

Nwadinigwe, C. A. and Okoroji, K. A. "Novel equations for quantitative hydrocarbon-type analysis of petroleum fractions." *Fuel*, 69, 340–343, 1990.

Riazi, M. R. and Daubert, T. E. "Prediction of molecular-type analysis of petroleum fraction and coal liquids." *Ind. Eng. Chem. Process.*, Des. Dev., 25, 1009–015, 1986.

Smith, H. M., U.S.Bureau of Mines, Tech. Paper, 1940.

Vakili-Nezhaad, G. R. and Modarress, H. "A new characterization factor of hydrocarbons and petroleum fluids fractions." *Oil & Gas Science and Technology* – Rev. IFP, 57, 2, 149–154, 2002.

Watson, K. M. and Nelson, E. F. "Improved methods for approximating critical and thermal properties of petroleum fractions." *Industrial Engineering Chemistry*, 25, 8, 880–887, 1933.

Case Study of Low Salinity Water Injection in Zichebashskoe Field

Abbas Zeinijahromi[a1], Vadim Ahmetgareev[b], Alexander Badalyan[a], Rais Khisamov[b] & Pavel Bedrikovetsky[a]

[a] Australian School of Petroleum, The University of Adelaide, Australia

[b] TATNIPINEFT Research Centre, Bugulma, Tatarstan, Russia

[1]abbas.zeinijahromi@adelaide.edu.au

Abstract

Low salinity waterflooding is a very promising EOR method in recent years. The mechanisms of enhanced recovery are considered to be decrease of residual oil saturation and alternation of rock wettability. In addition, the mobility control mechanism due to induced fines migration by low salinity water, and the consequent flux diversion is also a possible mechanism for enhanced recovery in low salinity waterflooding. The current paper analyzes production and injection history data from 24 years of production from Zichebashskoe field (Russia) which includes 7 years of low salinity water injection. The mathematical model for waterflooding with fines migration is applied for history matching. The result is a good agreement between the field history and modelling data. The Roxar tracer model is then used to compare recovery factor for two scenarios of low salinity water injection (field history) and conventional water injection using formation water (High salinity). The results shows insignificant incremental recovery (< 0.1%) and decrease in the amount of produced water during the development of Zichebashskoe field. It can be explained by the production of significant amount of the reservoir water (> 45% of total produced water) before the commencement of low salinity water injection and also injectors placing. A two layer cake reservoir is built using Zichebashskoe field permeability distribution to study the effect of low salinity water injection in a 5 spot pattern. Modeling results show significant improvement in oil recovery (~10%) and large reduction of water cut.

Keywords

Field Data; Low Salinity Waterflood; Fines-assisted Waterflooding; History Matching; Fines Migration

Introduction

Low salinity waterflooding is a recently developed EOR technique that improves mostly microscopic displacement efficiency by alternating the rock wettability towards more water wet. The detailed analysis of microscopic physics mechanisms of low salinity waterflooding is explained in details in the reviews by Morrow and Buckley, 2011 and Sheng, 2014. Recent studies of low salinity waterflooding have largely focused on the effects of water compositions on wettability, capillary pressure, relative permeability and residual oil saturation (Tang and Morrow, 1999; Yildiz and Morrow, 1996; Pu et al., 2010; Jerauld et al., 2008; Takahashi and Kovcsek, 2010; Berg et al., 2010; Cense et al., 2011; Mahani et al., 2011; Zhang and Morrow, 2006, Ibrahim et al., 2013). Above studies summaries the effects of low salinity waterflooding to be similar to that for chemical EOR methods (Lake, 1989).

Other effects of low salinity waterflooding on incremental oil recovery involve mobilization and migration of natural reservoir fines and consequent straining of pores (Zeinijahromi et al. 2014). Morrow and Buckley, 2011 suggest also that the formation of lamellae and emulsions, stabilized by fines, their migration and straining may result in mobility control and deep reservoir flow diversion. Tang and Morrow, 1999 and Fogden et al., 2011, suggest another mechanism of oil-wet and mixed-wet fines detachment by advancing water-oil capillary menisci; the resulting straining may also decrease the water relative permeability and increase oil recovery.

These effects appear to be separate phenomena from the fines lifted by low salinity water and plugging of water-filled pores, but may occur simultaneously with fines migration. Hussain et al, 2012 aimed to confirm the above effects of the water phase permeability reduction during high- and low-salinity waterflooding in oil-saturated rock. It was concluded that the water-wet particles have been removed from the rock by moving low salinity water, resulting in decrease in relative permeability for water and in increase in

2168-5517/15/01 016-16, © 2015 DEStech Publications, Inc.
doi: 10.12783/jpsr.2015.0401.03

fractional flow for oil. The conclusions agree with the above mechanisms proposed by Sarkar and Sharma, 1990.

Some low salinity core flood studies have reported the release of significant amounts of fines (Bernard, 1967; Tang and Morrow, 1999; Pu et al., 2010), while others showed no evidence of fines migration (Lager et al., 2008; Jerauld et al., 2008; Rivet et al., 2010) even though additional oil was recovered. In order to separate these effects, the injections leading to fines lifting and permeability decline are called in the current work "the fines-assisted waterflooding" (Kruijsdijk et al., 2011). The fines-assisted version of low salinity waterflooding is a mobility control EOR technology. The present paper only considers the effects of fines mobilization and capture to provide mobility control and does not consider changes to the residual oil saturation or relative permeability curves as a result wettability alternation during of injecting low salinity water.

The available literature on laboratory studies and mathematical modelling of low salinity waterflooding highly exceeds that on field trials. Very limited information on low salinity waterflooding pilot tests have been published in the open literature. Several limited field applications show significant recovery of residual oil (Webb et al., 2004; McGuire et al., 2005; Seccombe et al., 2010). However, the North Sea pilot, where the screening criteria for low salinity waterflood have been met, did not exhibit an incremental recovery (Skrettingland et al., 2010). The lack of information on real field applications of smart waterflooding with alteration of injected water composition as compared with the formation water is a serious restriction for large scale application of the technology in oil industry.

The paper presents analysis of a field case based on available production and injection data from the field under study. In the present paper we describe the results of 7 years of low salinity water injection in Zichebashskoe field (Russia, Tatarstan). The field production data is successfully history matched with fines-assisted mathematical model (see Zeinijahromi et al. 2014). Tempest reservoir simulator for fines-assisted low salinity waterflooding is used for the parameter tuning and adjustment of the static geologic reservoir model. Minor recovery enhancement and small reduction in injected water volume if compared with "normal" waterflooding is explained by production of significant amount of water before commencement of water flooding and by already high sweep efficiency during water injection into the aquifer.

The structure of the paper is as follows. First, we briefly describe the Zichebashskoe field and the history of oil and water production and low salinity water injection (Section 1). Section 2 presents the description of the reservoir model and the methodology of the history matching which is used. It follows by comparison between the low salinity waterflooding (field history) and "normal" waterflooding results (formation water injection) for the conditions of Zichebashskoe field. The analysis of the modelling results with possible explanation of low reservoir response to smart fines-assisted waterflooding concludes the paper.

Description of Low-salinity Waterflooding in Zichebashskoe Field

Figure 1 shows saturation map of the Zichebashskoe field in 2013. The wells' location are shown where the crossed circles symbols correspond to 8 injectors and the remaining are location of 29 producers.

The main injectors are located to inject water into the aquifer near water-oil contact.

The Zichebashskoe field consists of two sandstone reservoirs, Tula and Bobrik (Figure 1 a,b and c). The layers are isolated and there is no hydrodynamic interaction between the layers. Figure 2a shows average permeability distribution in two layers and in also four cross sections (Figure 2b) that are marked on the map in Figure 1. It can be observed that upper layer has higher horizontal connectivity and permeability.

Production from Zichebashskoe field started in 1989 followed by low salinity water injection in 2006. Water production curve on Figure 3 shows that a significant volume of water has already been produced before start of low salinity water injection in 2006. The injectors are located below water-oil contact and inject low salinity water in the water zone in order to provide pressure maintenance during 2006-2013. Figure 1 shows oil saturation averaged over the production thickness. The saturation map is obtained from 3D reservoir simulation after matching the

production and injection history up to end of 2013. Water cut in production wells gradually decreases from the position of initial oil-water contact up to the central part of the anticlinal field. One can also see that oil saturation increases from peripheral areas, where the injectors are located, towards the central part of the field.

The main properties of fluids and rocks are given in Table 1. The initial pressure is above the bubble point pressure; hence there is no initial gas cap and primary energy for the production is provided by adjacent active aquifer.

Table 2 and 3 show the formation and injected water compositions, respectively. Extremely high formation water salinity is defined by sodium chlorite concentration that highly exceeds those for other salts, while magnesium and calcium salts dominate in injected water. Thus, intensive ion exchange is expected during the displacement of formation water by injected water.

Water injection into aquifers yields better sweep and displacement than that in the oil zone, since the displacement of oil by water during the injection into aquifer is going on "by the plane surface" moving upwards water-oil contact (Lake, 1989, Bedrikovetsky, 1993). Slope of the peripheral zones near the initial water-oil contact also increases the recovery during bottom-up waterflooding, since gravity decelerates water and accelerated oil. The above explains high displacement efficiency.

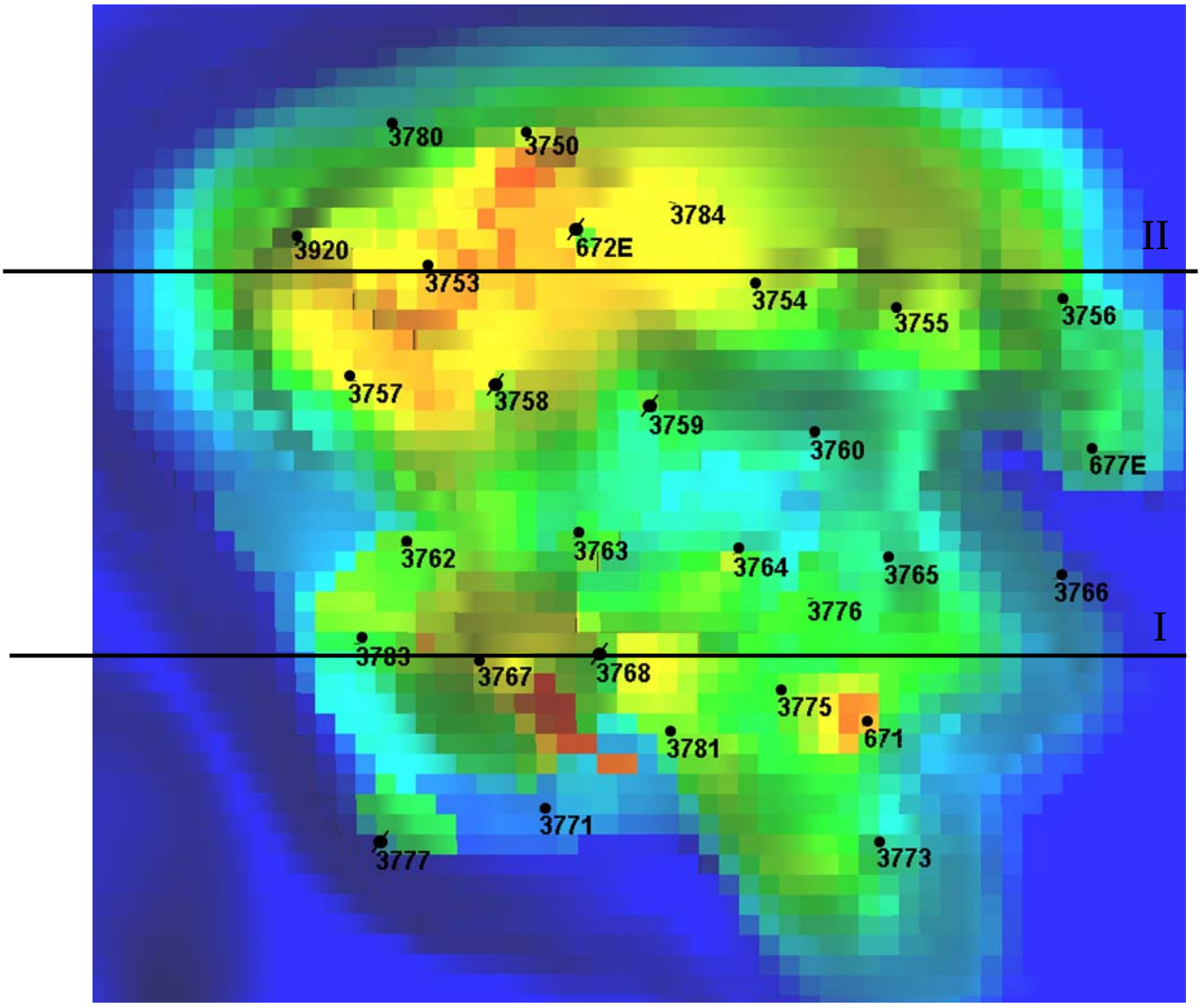

a)

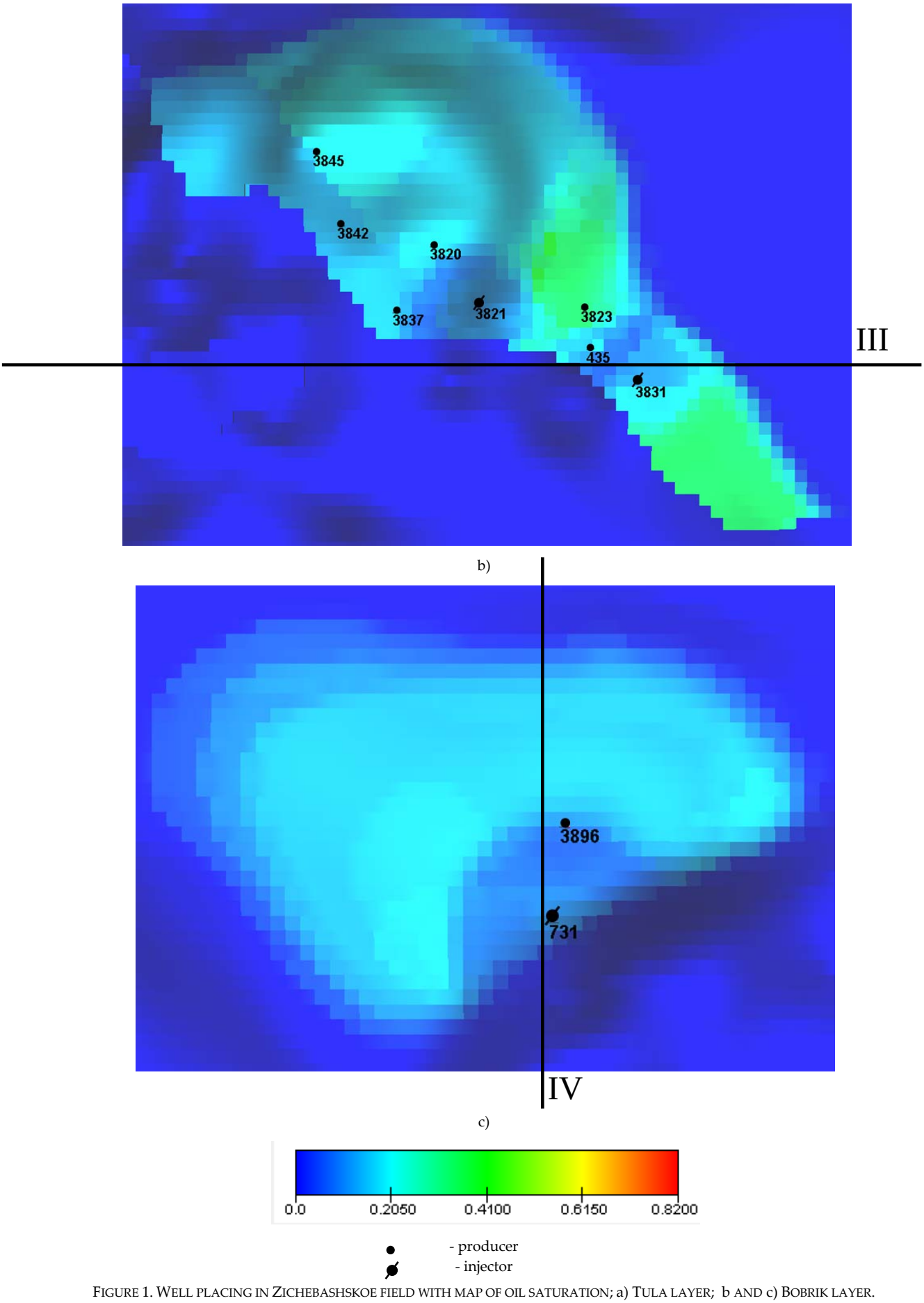

FIGURE 1. WELL PLACING IN ZICHEBASHSKOE FIELD WITH MAP OF OIL SATURATION; a) TULA LAYER; b AND c) BOBRIK LAYER.

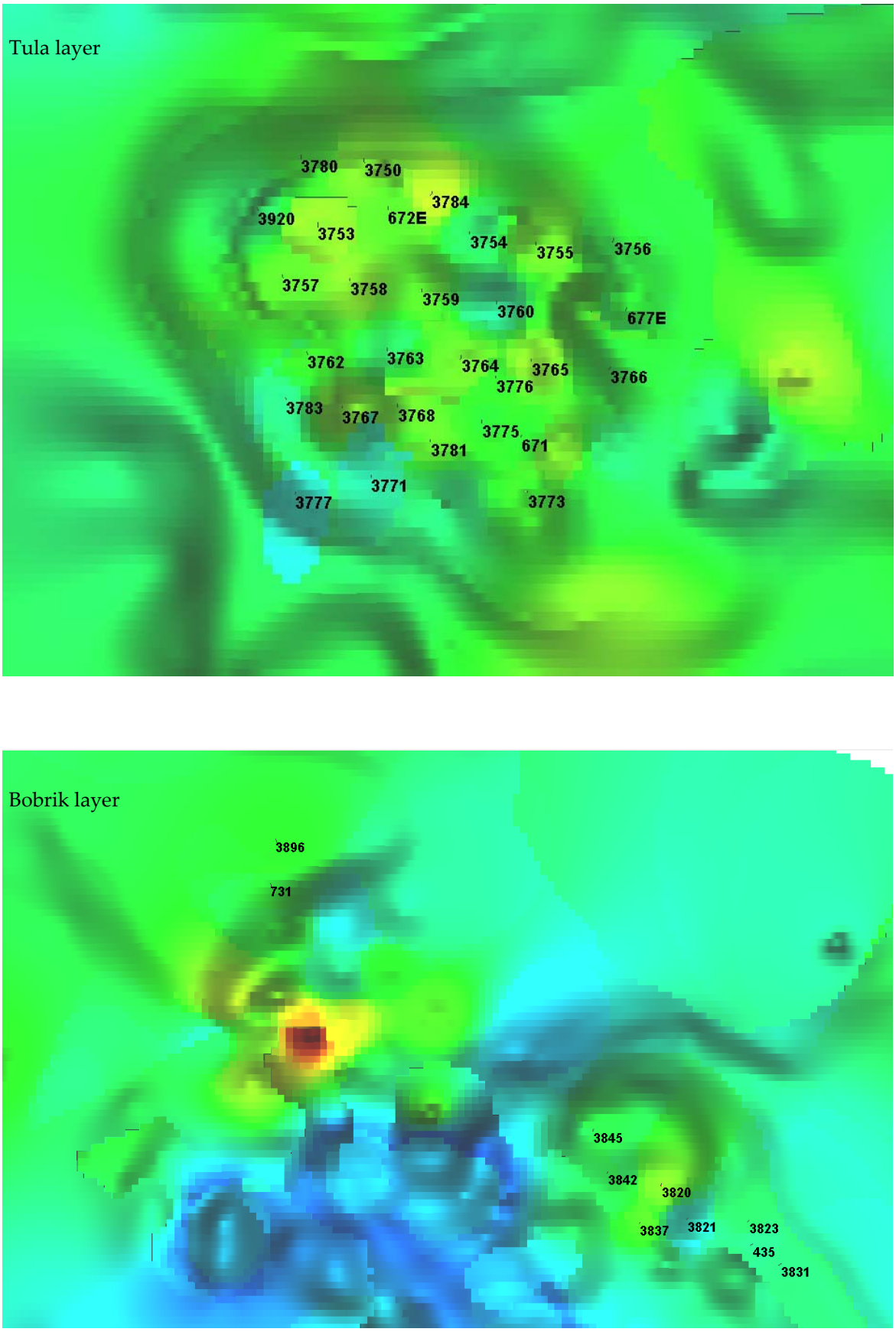
Tula layer
3780
3750
3784
3920
672E
3753
3754
3755
3756
3757
3758
3759
3760
677E
3762
3763
3764
3765
3766
3776
3783
3767
3768
3775
671
3781
3771
3777
3773
Bobrik layer
3896
731
3845
3842
3820
3837
3821
3823
435
3831

a)

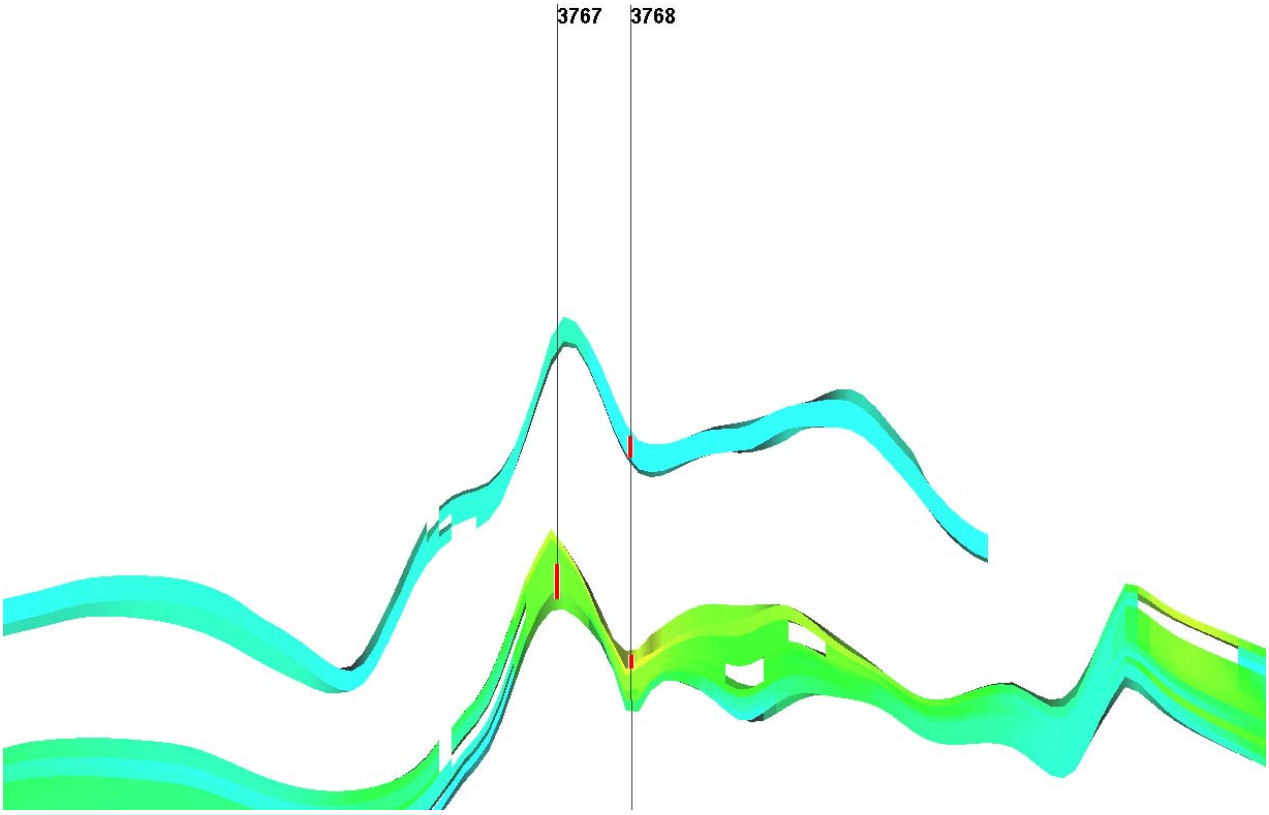

I

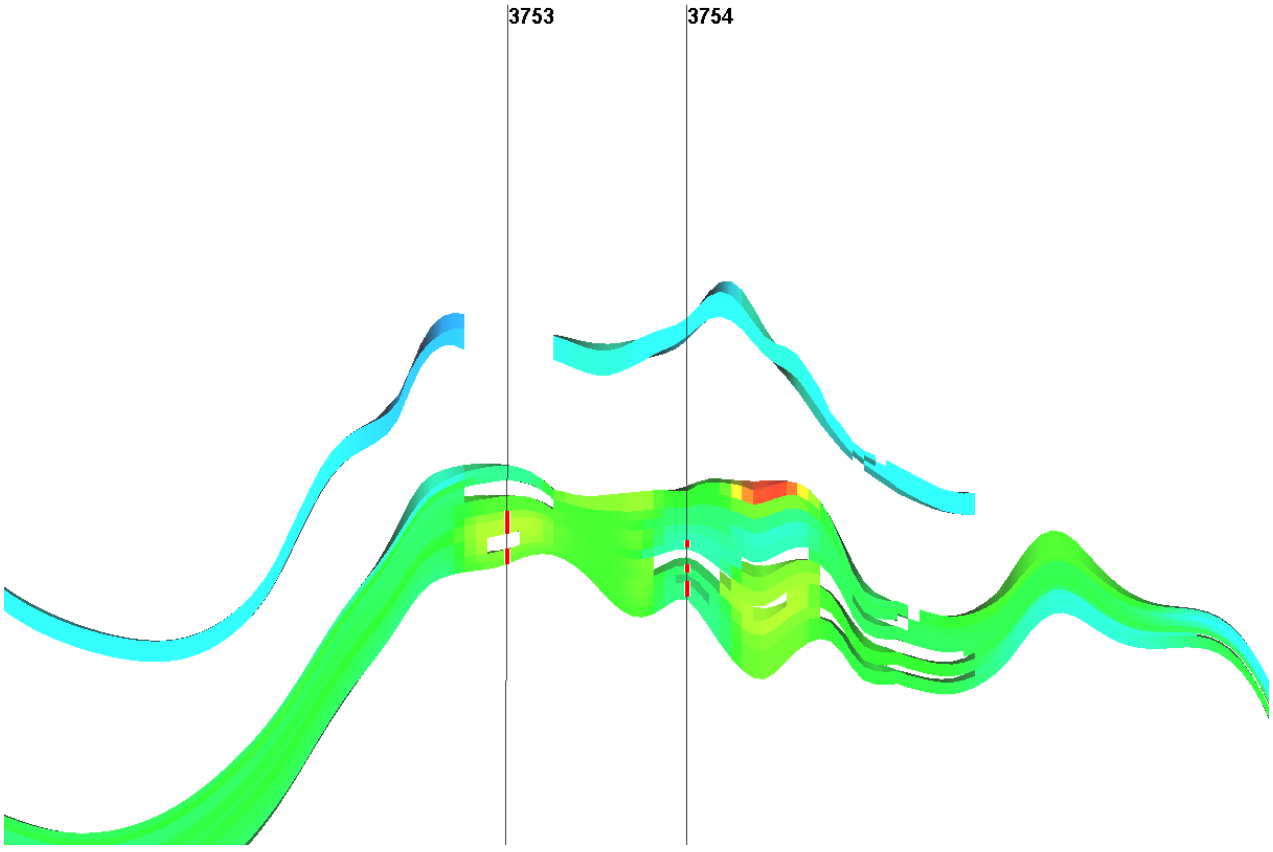

II

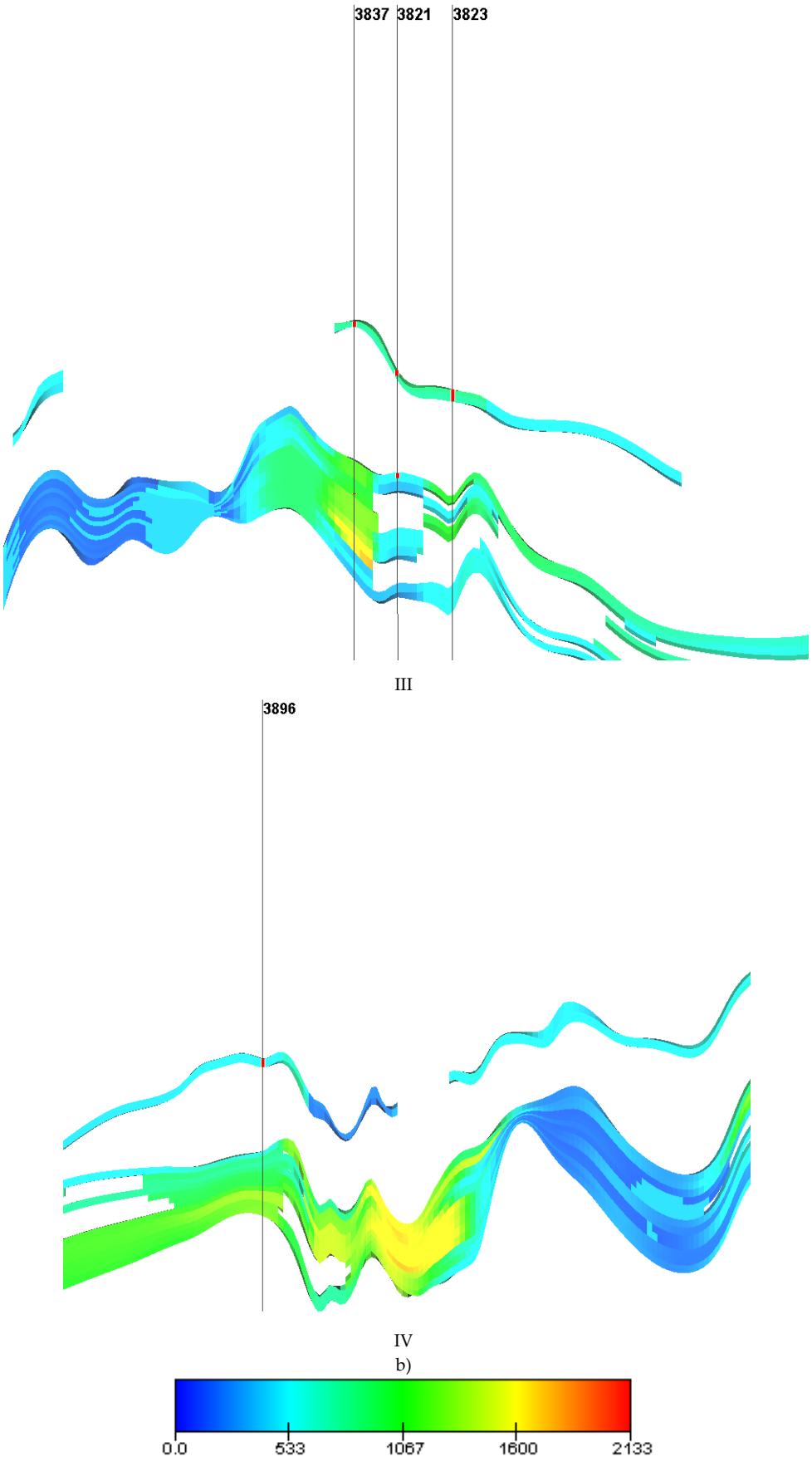

FIGURE 2. a) AVERAGE PERMEABILITY OF TULA AND BOBRIK LAYERS b) PERMEABILITY OF LAYERS IN CROSS SECTIONS OF THE FIELD; c)SCALE FOR PERMEABILITY IN mD.

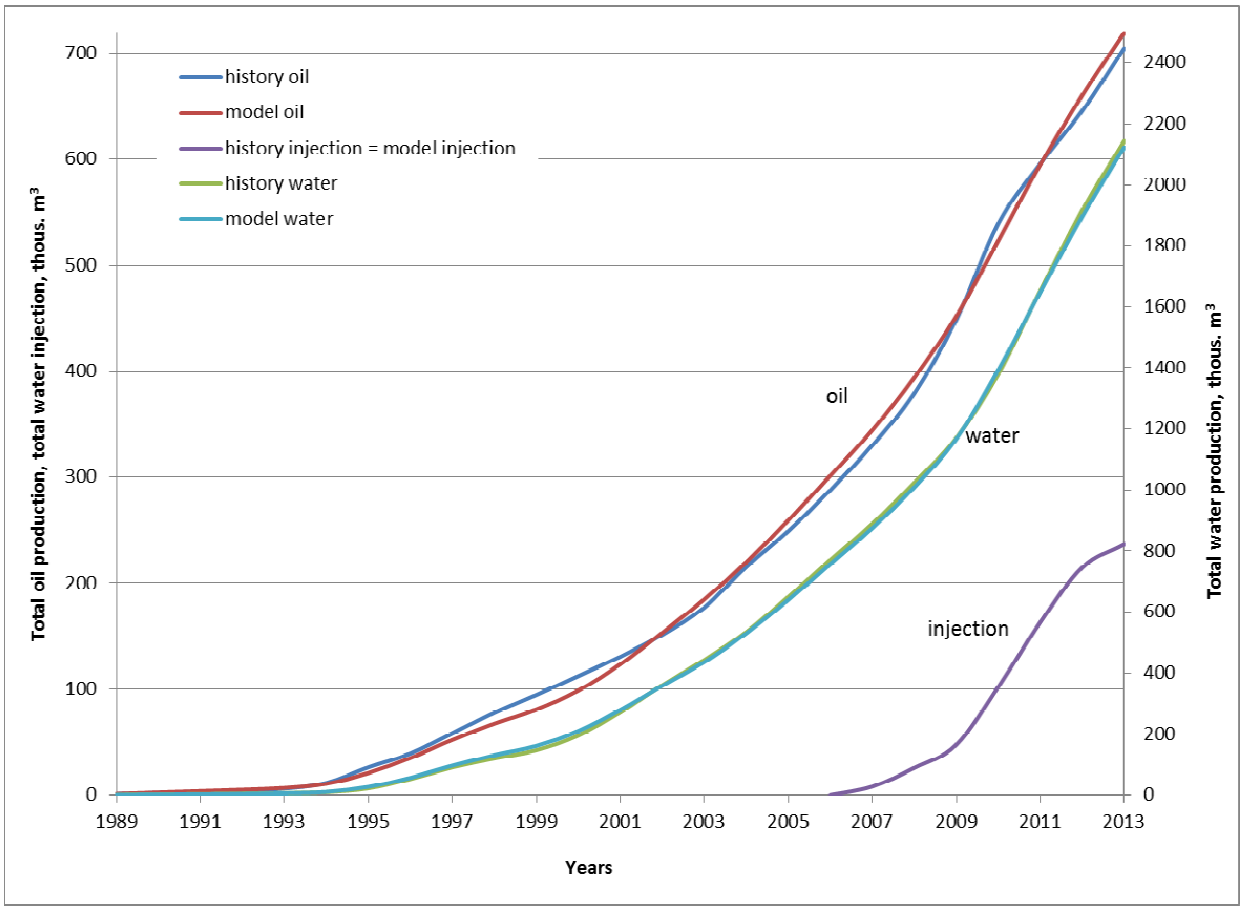

FIGURE 3. HISTORY MATCHING OF LOW_SAL WATERFLOODING: ACCUMULATED OIL PRODUCTION; ACCUMULATED WATER PRODUCTION; ACCUMULATED WATER INJECTION

TABLE 1. PROPERTIES OF ROCKS AND FLUIDS IN BASTRYKSKOYE FIELD.

Characteristic	Horizon, layer	
	Tulsky	Bobrikovsky
Reservoir top depth, m	1180	1200
Reservoir type	porous	porous
Formation thickness, m	2.3	11.5
Net pay thickness, m	1.8	4.3
Relative thickness of sandstone layers	0.98	0.93
Initial oil saturation	0.78	0.82
Reservoir temperature, ^{0}C	25	25
Initial reservoir pressure, MPa	11.8	12
Bubble point pressure, MPa	1.3	2.1
GOR, m^3/ton	1.7	1.4
Oil density under reservoir conditions, kg/m^3	875	870
Oil density under surface conditions, kg/m^3	880	883
Oil viscosity under reservoir conditions, mPa·s	26.6	21.5
Formation volume factor	1.039	1.023
Water density under reservoir conditions, kg/m^3	1170	1170
Water viscosity under reservoir conditions, mPa·s	1.7	1.7
Specific-productivity index, m^3/(day·MPa·m)	2.1	2.4
Displacement efficiency obtained from corefloods	0.572	0.600

TABLE 2. COMPOSITION OF FORMATION WATER IN ZICHEBASHSKOE FIELD.

Compound	MW g/mol	Conc. mol/L	Conc. mg/L	Conc. g/L	Conc. % (w/w)	Ionic strength mol/L
NaCl	58.439	3.40356	198900.5	198.9005	80.03	
$MgCl_2$	95.205	0.11935	11362.4	11.3624	4.57	
$MgSO_4$	120.367	0.00614	739.3	0.7393	0.30	4.79
$CaCl_2$	110.978	0.33684	37382.2	37.3822	15.04	
$NaHCO_3$	84.006	0.00172	144.6	0.1446	0.06	
				Total	**100.00**	

TABLE 3. COMPOSITION OF FRESH LAKE WATER INJECTED IN ZICHEBASHSKOE FIELD.

Compound	MW g/mol	Conc., mol/L	Conc., mg/L	Conc., g/L	Conc., % (w/w)	Ionic strength mol/L or M
NaCl	58.439	0.00034	20.1	0.0201	2.37	
$MgCl_2$	95.205	0.00029	28.1	0.0281	3.31	
$MgSO_4$	120.367	0.00115	137.8	0.1378	16.25	0.0179
$CaCl_2$	110.978	0.00250	276.9	0.2769	32.64	
$NaHCO_3$	84.006	0.00459	385.5	0.3855	45.44	
				Total	**100.00**	

Reservoir Simulation

The mathematical model for low-salinity waterflooding, where the incremental recovery is caused by the capillary phenomena and wettability alteration with the consequent decrease in residual oil saturation is similar to that of the chemical EOR (Lake, 1989). The basic equations include mass balances for oil, water and some ions. The equations for equilibrium ion exchange and sorption on clays give the ion sorption isotherms. The relative phase permeability and capillary pressure are ion-concentration-dependent.

If the incremental oil recovery is caused by lifting of attached fines, their migration and straining in thin pore throats, the model is similar to those of mobility control EOR. In the present study the comparison between the fines-assisted with low salinity water injection and normal waterflooding is performed for the field conditions. Therefore, the mathematical model for low salinity waterflood with changing relative phase permeability and accounting for fines mobilisation and straining, yielding permeability reduction in water swept areas, is used (see Zeinijahromi et al., 2013). The basic equations are mapped on the system of equations for polymer flooding, allowing above processes with low salinity water injection to be modeled using polymer option of black-oil model. Reservoir simulation software Tempest (Roxar 2014) is used for modelling of low salinity and "normal" waterflooding in this study. The tracer option in Tempest is equivalent to polymer option without adsorption, where relative permeability can be made dependent on tracer (salt) concentration. This option fits to fines assisted model for low salinity waterflooding. The tuning parameters are pseudo (at the reservoir scale) phase permeability for oil and formation water, and the reduction factor to obtain the phase permeability for low salinity water from the phase permeability for "normal" water. A good agreement between field history and modeling results

using fines assisted mathematical model (Tracer option in Tempest) can be seen in Figure 3.

The coreflood results presented in laboratory studies by Zeinijahromi et al., 2014 and Hussain et al., 2013 show that changing from injection of formation water to fresh water causes a significant decrease in relative permeability for water under residual oil saturation k_{rwor}; while residual oil saturation, connate water saturation and relative permeability for oil under connate water are almost the same.

The 5 folds decrease of k_{rwor} (reduction factor) is used in this study which is in agreement with that obtained in laboratory studies by Zeinijahromi et al., 2014 and Hussain et al., 2013.

The history matching procedure is a follows: The Corey form of pseudo relative permeability for each of two reservoirs is assumed. The pseudo relative permeability k_r depends on saturation (s) and salinity (γ): $k_{rj}=k_{rj}(s,\gamma)$, j=W,O. Following the coreflood studies by Hussain et al., 2013, it is assumed that pseudo relative permeability for oil, residual oil saturation and power for oil (n_o) are independent of salinity. The value of end point relative permeability k_{rwor} for injected salinity (γ=0) is assumed to be five times lower than that for formation water (γ=1).

The Corey parameters are obtained by tuning the curves of cumulative oil and water production. The form of tuned pseudo relative permeability is shown in Figure 4a for Tula layer and in Figure 4b for Bobrik layer.

The obtained Corey parameters for oil-formation water are shown below Figures 4a and 4b. The Corey powers smaller than unity determine the convex forms of pseudo phase permeability, which is typical for those as obtained at the reservoir scale.

The result of history matching is presented in Figure 3 that exhibits a good match between the field history and the modelling data after the history matching. This model is later used to simulate normal (formation) water injection scenario in order to compare with the 7 years history of low salinity water injection in Zichebashskoe field.

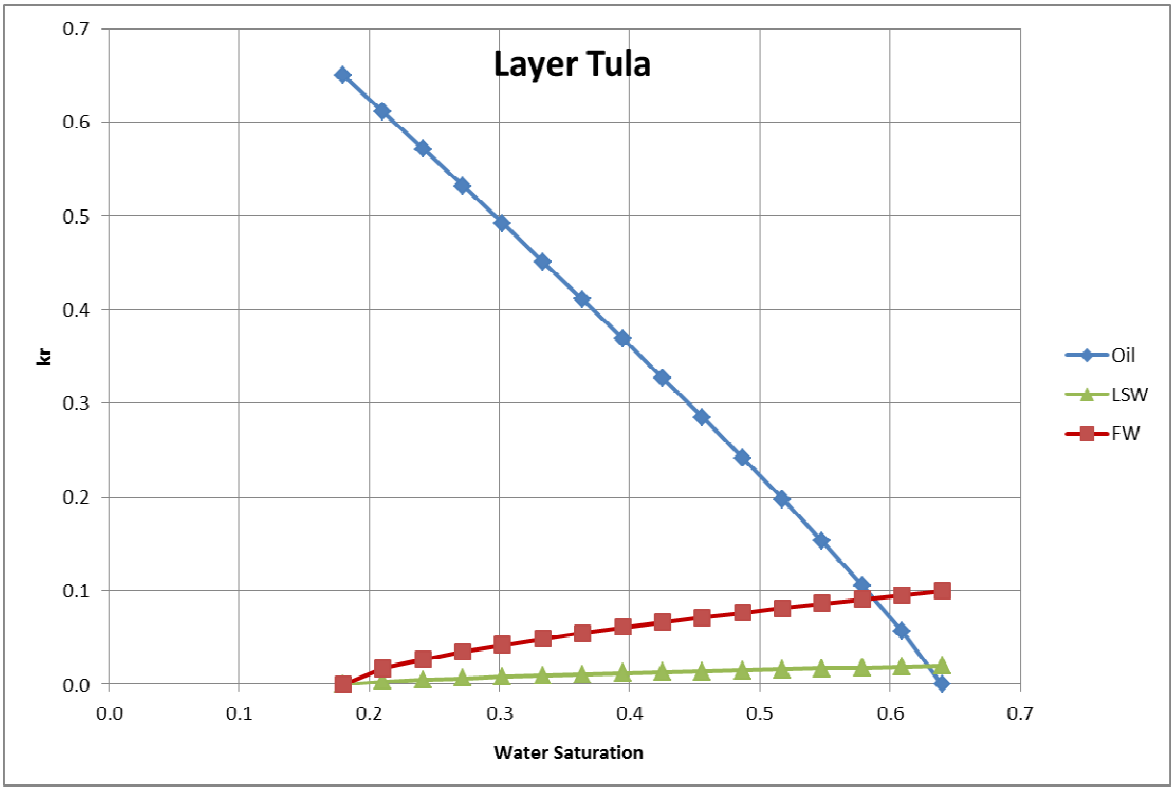

Swi	Sor	Krowi	Krwor	Nw	No
0.18	0.36	0.65	0.100	0.65	0.9

a)

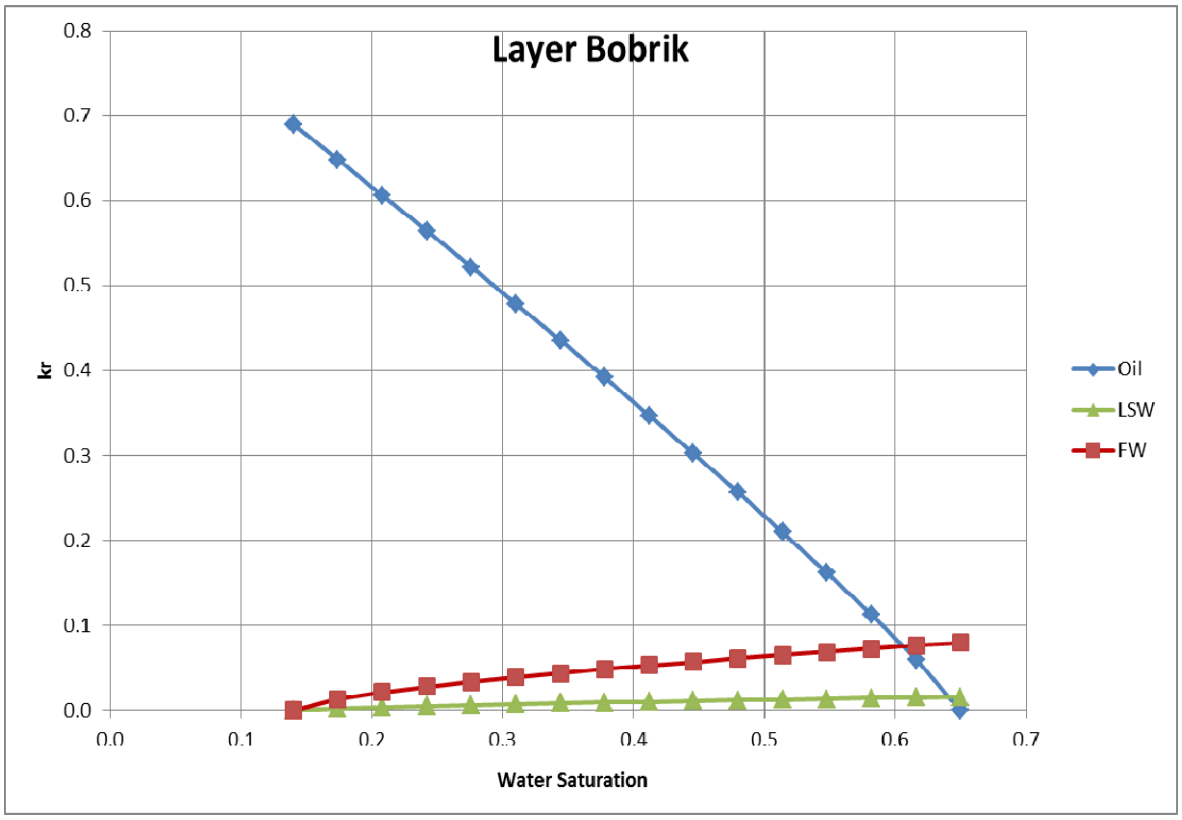

Swi	Sor	Krowi	Krwor	Nw	No
0.14	0.35	0.69	0.080	0.65	0.9

b)

FIGURE 4. PSEUDO RELATIVE PERMEABILITY: a) TULA LAYER; b) BOBRIK LAYER.

Comparison between Normal and Low-salinity Waterfloods in Zichebashskoe Field

The purpose of this section is to back calculate the recovery from the reservoir if formation water had been injected and compare it with field history that is low salinity water injection. Experimental results from different studies showed that during the injection of formation water, no ionic exchange or fines migration due to alteration of electrostatic force occur. Therefore, we define formation water injection as a basic waterflood option, which is referred to as "normal" waterflooding. Figure 5 shows the comparison for water cut and recovery factor between the normal and low salinity waterflooding. The incremental recovery factor due to injection of low salinity water is less than 1% and almost causes no change in produced water.

In order to study the effect of well placing pattern on fines assisted methods of EOR, a comparative study is performed for a 5 spot pattern in a two layer cake reservoir with similar heterogeneity to Zichebashskoe field as described in Zeinijahromi et al., 2014.The results of low salinity water injection in two-layer 5-spot pattern with size 200x200 m during 1400 days (4 years) are presented in Figure 6. The layer properties, including pseudo phase permeability are the same as that in Tula and Bobrik layers (Figure 4 a,b). Following Hussain et al. 2013 it is assumed that Low salinity of injected water causes 5-fold decrease in relative permeability for water. It causes large incremental recovery factor of 11% and significant reduction in water production that agrees with the results reported in Zeinijahromi et al., 2014. A higher incremental recovery obtained from 5-spot pattern if compared with injection into WOC in Zichebashskoe field is majorly due to commencement of low salinity water injection from start of production and injector locations.

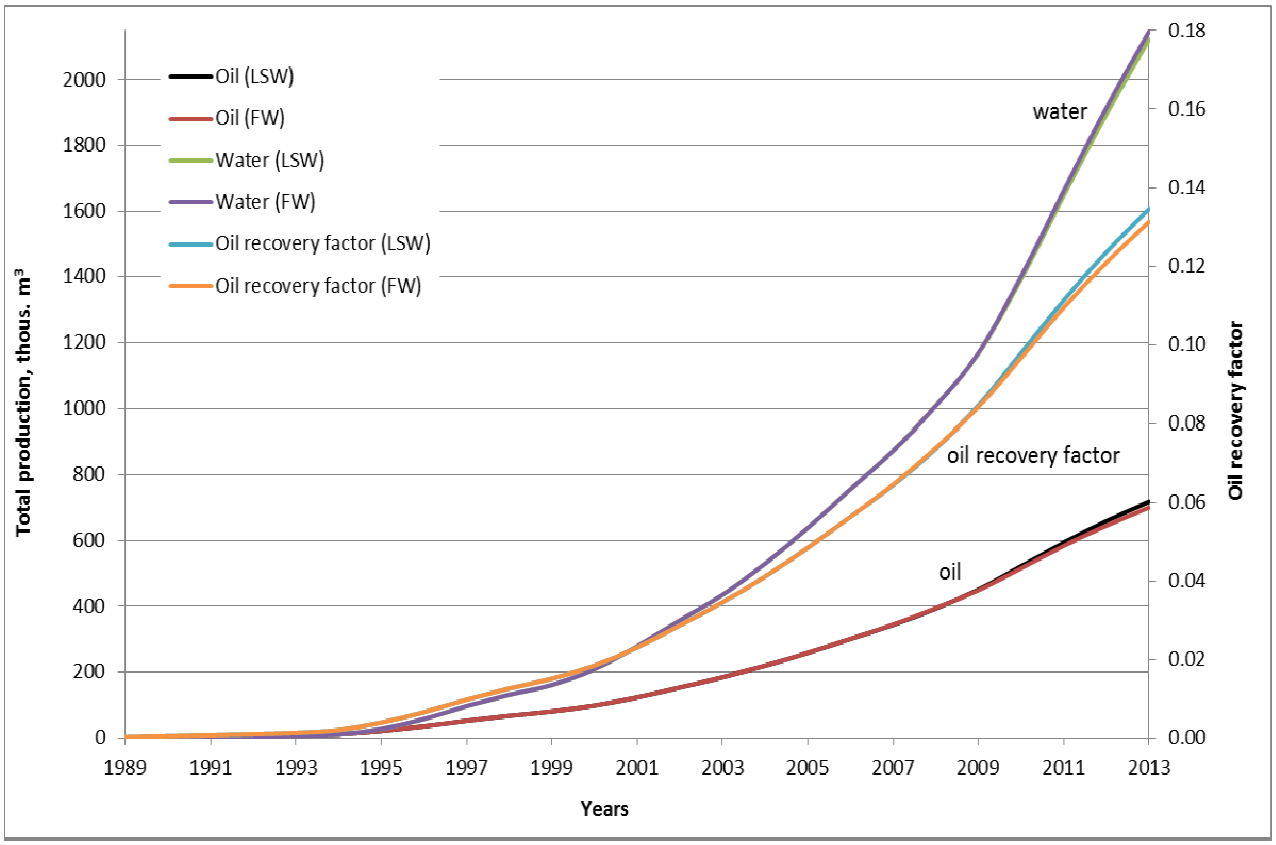

FIGURE 5. COMPARISON BETWEEN INJECTIONS OF LOW SALINITY AND HIGH SALINITY WATERS FOR CONDITIONS OF ZICHEBASHSKOYE FIELD.

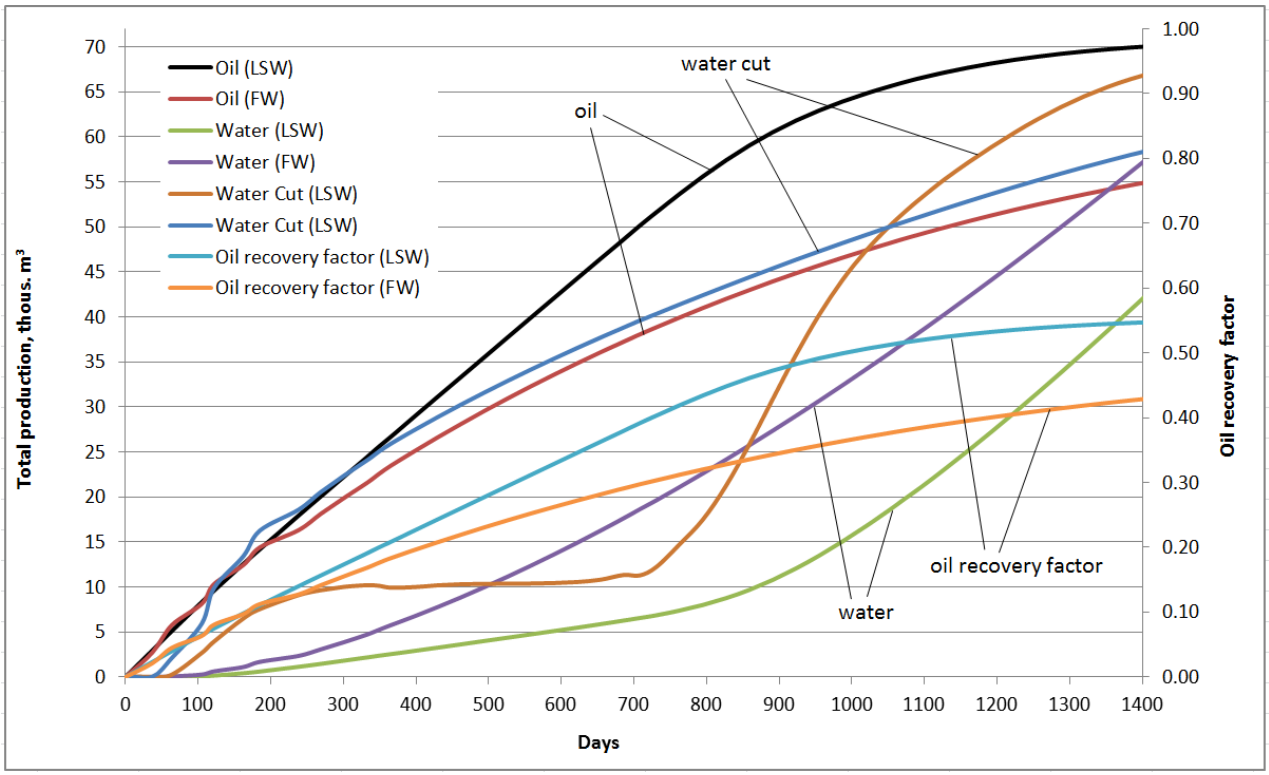

FIGURE 6. COMPARISON BETWEEN INJECTIONS OF LOW SALINITY AND HIGH SALINITY WATERS FOR TWO-LAYER CAKE RESERVOIR (WITH ZICHEBASHSKOYE FIELD'S CHARACTERISTICS), 5-SPOT PATTERN 200X200 M.

Summary and Discussions

The objective of the present work is preliminary analysis of low salinity waterflooding in the Zichebashskoe oil field and its comparison with the normal (formation) waterflooding. It is assumed that low salinity waterflooding causes fines migration and induces permeability damage in the water swept areas, resulting in deep reservoir flux diversion.

The tuned pseudo relative permeability has typical convex form, which is typical for up scaled relative permeabilities at the reservoir length scale. The 5-folds decrease of relative permeability for water due to salinity decrease is typical for sandstone reservoir cores (see Hussein et al., 2013).

The tuned reservoir model shows very little recovery increment and small reduction in produced water for low salinity fines-assisted waterflooding if compared with injection of formation water. However, these effects for injection into 5-spots pattern are significant. It can be explained by significant amount of water that has been produced before the injection in Zichebashskoe field, i.e. the injected water displaces the oil under high water saturation. The water-cut map shows that the sweep by the low salinity water is minimal due to water injection into the aquifer, almost no low salinity water was produced (Figure 1). The central part of the reservoir is poorly swept by the injected water. Oil is directly displaced by high salinity formation water, injected water lags significantly behind. The above is the main reason why the incremental recovery factor with low salinity waterflooding is not high.

Sweep efficiency for water injection into aquifer is higher than that with the injection into oil zone. The discussed fines-assisted low salinity waterflood mostly affects the sweep, which is already high. This is another reason why low salinity fines-assisted waterflood does not exhibit high incremental recovery in the case under consideration while in 5 spot patterns it results in significant improvement of sweep.

The model for low salinity waterflood only accounts for fines migration and consequent decrease of relative permeability for water, i.e. the effects of wettability change and residual oil saturation decreasing are ignored. Accounting for decrease in relative permeability for oil and decrease in oil residual can bring additional incremental recovery if compared with the normal waterflooding. This study lacks the laboratory coreflooding and determining the relative phase permeability for formation and injected waters.

Both effects of sweep and of better displacement coefficient can affect only the boundary wells. The central part of the reservoir will be affected at the later stage, when the boundary wells are watered out and abandoned, and central wells will produce injected water.

The problem whether in general the incremental recovery with low salinity waterflood in both chemical EOR and mobility-improvement modes during the injection into aquifer is low, may be a subject of additional investigation.

Only very limited information from the field is available; hence, significant amount of additional investigations (coreflooding, SEM, XRD) must be performed for detailed analysis of the Zichebashskoe field case.

Conclusions

Oil and water production data for low salinity waterflooding in Zichebashskoe oilfield can be matched by the fines-assisted-waterflood model (tracer model in Roxar) with high accuracy.

Low salinity water injection under the conditions of Zichebashskoe field results in less than 0.1% improvement in incremental recovery and low decrease in the produced water if compared with 10% incremental recovery from waterflooding by formation water under 5-fold decrease in relative permeability for water due to induced fines migration.

The phenomenon is explained by high flooding of the reservoir before commencement of low salinity water injection, by high salinity water which includes almost 45% of total water production. Another explanation is: low salinity water injection into aquifer causes lower incremental recovery than that with the injection into oil-zone.

REFERENCES

Bedrikovetsky, P., (1993). Mathematical Theory of Oil & Gas Recovery, Kluwer Academic Publishers, London-Boston-Dordrecht, 600 p.

Bedrikovetsky, P., Zeinijahromi, A., Siqueira, F., Furtado, C.

and Souza, A., (2011). Particle detachment under velocity alternation during suspension transport in porous media. *J. Transport in Porous Media*: , v. 91 (1), p. 173-197..

Bedrikovetsky, P.G., Vaz, A., Machado, F., Zeinijahromi, A., Borazjani, S., 2012, Skin due to Fines Mobilisation, Migration and Straining during Steady State Oil Production, J Petrol Sci Tech, 30:15, 1539-1547

Berg, S., Cense, A.W., Jansen, E. and Bakker, K., 2010. Direct Experimental Evidence of Wettability Modification by Low Salinity. Petrophysics 52 (5): 314-322. doi: 2010-v51n5a3.

Bernard, G.G., 1967. Effect of Floodwater Salinity on Recovery of Oil from Cores Containing Clays. Paper SPE 1725 presented at the SPE California Regional Meeting, Los Angeles, California, USA, 26-27 October.

Chauveteau, G., Nabzar, L. and Coste, J., (1998). Physics and Modeling of Permeability Damage Induced by Particle Deposition. SPE 39463. *SPE Formation Damage Control Conference*: 409-419.

Cense, A., Berg, S., Bakker, K. and Jansen, E., 2011. Direct Visualization of Designer Water Flooding in Model Experiments. Paper SPE-144936-MS presented at the SPE Enhanced Oil Recovery Conference, Kuala Lumpur, Malaysia, 19-21 July.

Civan, F., (2007). Reservoir Formation Damage: fundamentals, modeling, assessment, and mitigation. Gulf Professional Publishing, Elsevier, Burlington, 1114 pp.

Civan, F., (2010). Non-isothermal Permeability Impairment by Fines Migration and Deposition in Porous Media including Dispersive Transport. *J. Transport in Porous Media*, 85(1): 233-258.

Fogden, A., Kumar, M., Morrow, N.R. and Buckley, J.S., 2011. Mobilization of Fine Particles During Flooding of Sandstones and Possible Relations to Enhanced Oil Recovery. Energy & Fuels 25 (4): 1605-1616.

Freitas, A. and Sharma, M., (2001). Detachment of particles from surfaces: an AFM study. *J. of Colloid and Interface Science*, 233(1): 73-82.

Jerauld, G., Webb, K., Lin, C. and Seccombe, J., 2008. Modeling Low-Salinity Waterflooding. SPE Res Eval & Eng 11 (6): 1000-1012.

Hussain, F., Zeinijahromi, A., Bedrikovetsky, P., Cinar, Y., Badalyan, A., Carageorgos, T., 2013, An Experimental Study of Improved Oil Recovery through Fines-Assisted Waterflooding, Journal of Petroleum Science and Engineering v. 109, p. 187-197.

Ibrahim, M, Jia, H, Nasr-El-Din,H., 2013. Effect of Brine Composition on CO2/Limestone Rock Interactions during CO2 Sequestration, Journal of Petroleum Science Research v. 2, p.14-26

Khilar, K. and Fogler, H., 1998. Migrations of Fines in Porous Media. Dordrecht/London/Boston: Kluwer Academic Publishers.

Lager, A., Webb, K., J. Black, C., Singleton, M. and Sorbie, K., 2008. Low Salinity Oil Recovery-an Experimental Investigation1. Petrophysics 49 (1): 28-35. doi: 2008-v49n1a2.

Lake, L., 1989. Enhanced Oil Recovery. New Jersy: Prentice-Hall.

Lemon, P., Zeinijahromi, A., Bedrikovetsky, P. and Shahin, I., 2011. Effects of Injected-Water Salinity on Waterflood Sweep Efficiency through Induced Fines Migration. Journal of Canadian Petroleum Technology 50 (9): 82-94.

Ligthelm, D.J., Gronsveld, J., Hofman, J., Brussee, N., Marcelis, F. and Linde, H.v.d., 2009. Novel Waterflooding Strategy by Manipulation of Injection Brine Composition. Paper SPE-119835-MS presented at the EUROPEC/EAGE Conference and Exhibition, Amsterdam, The Netherlands, 8-11 June.

Mahani, H., Sorop, T., Ligthelm, D.J., Brooks, D., Vledder, P., Mozahem, F. and Ali, Y., 2011. Analysis of Field Responses to Low-Salinity Waterflooding in Secondary and Tertiary Mode in Syria. Paper SPE 142960 presented at the SPE EUROPEC/EAGE Annual Conference and Exhibition, Vienna, Austria, 23-26 May.

Mojarad, R. and Settari, A., (2007). Coupled Numerical Modelling of Reservoir Flow with Formation Plugging. *J. of Canadian Petroleum Technology*, 46(3): 54-59.

Mojarad, R. and Settari, A., (2008). Velocity-based Formation Damage Characterization Method for Produced

Water Re-injection: Application on Masila Block Core Flood Tests. *J. Petroleum Science and Technology*, 26(7): 937-954.

Morrow, N. and Buckley, J., 2011. Improved Oil Recovery by Low-Salinity Waterflooding. Journal of Petroleum Technology 63 (5): 106-112.

Nabzar, L., Chauveteau, G. and Roque, C., (1996). A New Model for Formation Damage by Particle Retention. SPE 1283. *SPE Formation Damage Control Symposium*.

Pu, H., Xie, X., Yin, P. and Morrow, N., 2010. Low-Salinity Waterflooding and Mineral Dissolution. Paper SPE 134042 presented at the SPE Annual Technical Confrence and Exhibition, Florence, Italy, 19-22 September.

Rousseau, D., Latifa, H. and Nabzar, L., (2008). Injectivity Decline From Produced-Water Reinjection: New Insights on In-Depth Particle-Deposition Mechanisms. *SPE Prod & Oper*, 23(4): 525-531.

Roxar. 2014 ©Emerson Roxar 1999-2014. http://www2.emersonprocess.com/en-US/brands/roxar/Pages/Roxar.aspx.

Sarkar, A. and Sharma, M., 1990. Fines Migration in Two-Phase Flow. Journal of Petroleum Technology 42 (5): 646-652. doi: 10.2118/17437-PA.

Schembre, J. and Kovscek, A., 2005. Mechanism of Formation Damage at Elevated Temperature. Journal of Energy Resources Technology 127 (3): 171-180. doi: 10.1115/1.1924398.

Schlumberger Information Solutions (SIS), 2010. Eclipse Reservoir Engineering Software. Schlumberger Limited. Available Online.

Seccombe, J., Lager, A., Jerauld, G., Jhaveri, B., Buikema, T., Bassler, S., Denis, J., Webb, K., Cockin, A., and Fueg, E. 2010. Demonstration of Low-Salinity EOR at Interwell Scale, Endicott Field, Alaska. Paper SPE 129692 presented at SPE/DOE Improved Oil Recovery Symposium, Tulsa, 24–28 April.

Sharma, M.M. and Yortsos, Y.C., (1987a). Transport of particulate suspensions in porous media: Model formulation. *AIChE Journal*, 33(10): 1636-1643.

Sharma, M.M. and Yortsos, Y.C., (1987b). A network model for deep bed filtration processes. *AIChE Journal*, 33(10): 1644-1653.

Sharma, M.M. and Yortsos, Y.C., (1987c). Fines migration in porous media. *AIChE Journal*, 33(10): 1654-1662.

Sheng, J., J. 2014. Critical reviewoflow-salinitywaterflooding. J. Petroleum Science and Engineering, 120, 216–224.

Skrettingland, K., Holt, T., Tweheyo, M.T., and Skjevrak, I. 2010. Snorre Low Salinity Water Injection—Core Flooding Experiments And Single Well Field Pilot. Paper SPE 129877 presented at the SPE/DOE Improved Oil Recovery Symposium, Tulsa, 24–28 April.

Takahashi, S. and Kovscek, A.R., 2010. Wettability Estimation of Low-Permeability, Siliceous Shale Using Surface Forces. Journal of Petroleum Science and Engineering 75 (1-2): 33-43.

Tang, G. and Morrow, N., 1999. Influence of Brine Composition and Fines Migration on Crude Oil/Brine/Rock Interactions and Oil Recovery. Journal of Petroleum Science and Engineering 24 (2-4): 99-111.

Webb, K.J., Black, C.J.J., and Al-Ajeel, H. 2004. Low Salinity Oil Recovery—Log-Inject-Log. Paper SPE 89379 presented at the SPE/DOE Symposium on Improved Oil Recovery, Tulsa, 17–21 April.

Yildiz, H. and Morrow, N., 1996. Effect of Brine Composition on Recovery of Moutray Crude Oil by Waterflooding. Journal of Petroleum Science and Engineering 14 (3-4): 159-168. doi: 10.1016/0920-4105(95)00041-0.

Yuan, H. and Shapiro, A.A., 2011. Induced Migration of Fines During Waterflooding in Communicating Layer-Cake Reservoirs. Journal of Petroleum Science and Engineering 78 (3–4): 618-626.

Yuan, H. and Shapiro, A., (2010a). Modeling non-Fickian transport and hyperexponential deposition for deep bed filtration. *Chemical Engineering J.*, 162(3): 974-988.

Yuan, H. and Shapiro, A., (2011). A Mathematical Model for Non-monotonic Deposition Profiles in Deep Bed Filtration Systems. *Chemical Engineering J.*, 166(1): 105-115.

H. Yuan, X. Zhang, A. A. Shapiro & E. H. Stenby (2014). Crossflow and Water Banks in Viscous Dominant Regimes of Waterflooding. *J. of Petroleum Science and Technology*, 32(10): 1227-1232.

Zhang, Y. and Morrow, N.R., 2006. Comparison of Secondary

and Tertiary Recovery with Change in Injection Brine Composition for Crude Oil/Sandstone Combinations. Paper SPE-99757-MS presented at the SPE/DOE Symposium on Improved Oil Recovery, Tulsa, Oklahoma, USA, 22-26 April.

Zeinijahromi, A., Lemon, P., Bedrikovetsky, P. 2011. Effects of Induced Migration of Fines on Water Cut during Waterflooding, Journal of Petr Sci Eng v. 78, p. 609-617

Zeinijahromi, A., Nguyen, T. K. P., Bedrikovetsky, P., 2013, Mathematical Model for Fines Migration Assisted Waterflooding with Induced Formation Damage, Journal of Society of Petroleum Engineers SPEJ, v.18(3) June, p. 518-533.

Zeinijahromi, A., Bedrikovetsky, P. 2014. Enhanced Waterflooding Sweep Efficiency by Induced Formation Damage in Layer-Cake Reservoirs: Laboratory Study and Mathematical Modeling, SPE-168203-MS, SPE International Symposium & Exhibition on Formation Damage Control, Lafayette, LA, USA, 26 – 28 February.

Zinati, F. F. , Farajzadeh, R. , Currie, P. K. and Zitha, P. L. J.(2009). 'Modeling of External Filter Cake

Build-up in Radial Geometry, *J of Petroleum Science and Technology*, 27: 7, 746 — 763.

Surfactant Preflood to Improve Waterflooding Performance in Bakken Shale Formation

Samiha Morsy*[1], J.J. sheng[2]

Bob L. Herd Department of Petroleum Engineering, Texas Tech University, Lubbock, Texas, USA

*[1]samiha.morsy@ttu.edu; [2]james.sheng@ttu.edu

Abstract

The lower primary oil recovery from shale formations accelerated the application of waterflooding technology as a secondary recovery mechanism at an earlier time compared with conventional reservoirs. This situation suggests the EOR surfactant technology designed to promote additional oil recovery from fractured carbonate formations is a fit for these shale formations that are characterized by complex fractured lithology. The presented study investigates the idea of incorporating appropriate surfactant formulations at a low dosage as a preflood to waterflooding in shale formations. If properly designed, such surfactant in the preflood fluid will penetrate into the high oil saturation matrix or natural fracture region and accelerate the extraction of the oil in place by rapid imbibition. This extracted oil can readily move from the matrix into the propped fracture system, and then be produced. Another benefit of the preflood surfactant is that it is engineered in such a way that it leaves the matrix or natural fracture face water wet to facilitate oil movement during production.

This paper presents a study of a series of surfactant additives developed for extracting additional oil. Over 10 of these specially customized product blends were evaluated in the laboratory for their effectiveness in increasing oil recovery of Bakken formation. Only one surfactant (Stim aid A) was compatible with Bakken formation brine and crude oil, so it was the only one used for spontaneous imbibition experiments. The average porosity of the used Bakken reservoir samples was 5.8% with an average bulk density of 2.75 g/cc. The Bakken rock samples were pre-treated with different surfactant solutions and then used for water spontaneous imbibition experiments. During the spontaneous imbibition, the maximum oil recovery was from the samples that were pre-treated with 2 wt.% of (Stim aid A) surfactant. The measured contact angles on Bakken samples showed an alteration in rock wettability that interpreted the improvement of Bakken higher recovery factors from spontaneous imbibition in surfactant solutions compared with brine solutions only.

Keywords

Surfactant Flooding in Bakken Shale; Waterflooding Improvement in Bakken Shale

Introduction

The United States holds about six trillion barrels of shale oil (Killen 2011). With higher oil prices, shale oil and gas are of great interest, especially in North America. Oil and gas shale formations vary in composition even within the same place due to the higher level of heterogeneity of these rocks. Shales contain roughly less than 10% organic, less than 50% clay, and the remainder is mostly quartz or calcite. In shale reservoirs, oil is stored in a very tight matrix with virtually all permeability concentrated in a large number of natural fractures (Fakcharoenphol et al. 2012). Due to these fractures, oil cannot be displaced from the matrix by means of conventional waterflooding. Channelling and bypassing through the fractures would result in extremely poor recovery (Guo et al. 1998). Primary oil production from such fractured reservoirs in which storage occurs in the matrix and fractures can be divided into three stages: 1) production from the fracture network at an early time; 2) production from the fracture network and rock matrix at an intermediate time; and 3) production from the rock matrix at a later time (Guo et al. 1998). Waterflooding usually starts during the mature stage of primary production in which production is dependent mainly on matrix permeability. Most of the recovery in this stage depends on spontaneous imbibition of brine into the rock matrix and expulsion of oil via the fracture face. Spontaneous imbibition can add a significant amount of oil recovery in fractured reservoirs with low matrix permeability depending on rock wetness quality.

Many surfactants recently have been proposed to enhance initial production in shale oil and gas formations. These surfactants are injected along with fracturing fluids to lower interfacial tension and alter rock wettability. Wang et al. (2011) studied the potential of different surfactant formulations to imbibe into and displace oil from shale core samples from the

2168-5517/15/01 032-06, © 2015 DEStech Publications, Inc.
doi: 10.12783/jpsr.2015.0401.04

middle member of the Bakken formation while minimizing clay swelling and formation damage in the formation. The range of recovery factors measured during their study were 1.55 to 76% OOIP at high salinity (150−300 g/L or15−30 wt.%) and temperatures ranging from 73−248°F using brine and surfactant (0.05−0.2 wt.% concentration). The best surfactants based on their study were ethoxylate nonionic surfactant, an internal olefin sulfonate anionic surfactant, and an amine oxide cationic surfactant as they were more stable than the other surfactants for temperatures from 221−248°F.

Another study by Xu and Fu (2012 a&b) showed that using weakly emulsifying surfactant is more efficient in solubilizing and mobilizing oil globules than a non-emulsifying surfactant in order to enhance initial production from the Eagle Ford shale formation. Paktinat et al. (2006) pointed out from the experimental and field case that a microemulsion accelerated post fracturing fluid cleanup in tight shale formations and resulted in lowering pressure to displace injected fluids from low permeability core samples and proppant packs. The authors mentioned that when 0.2 wt.% of microemulsion was used, gas relative permeability increased and as a result water permeability decreased. They believed that the frac fluid effectively lowered the capillary pressure and capillary end effect associated with fractures in shales as much as 50%, thus minimizing fluid trapping and increased the flow area to the fracture (longer frac half-length).

Fernø, Haugen, and Graue, 2012 presented an experimental study on carbonate reservoirs showing that surfactant prefloods helped water flooding efficiency by lowering the capillary threshold pressure for water to invade the matrix pores that makes the transport of water much easier between the matrix and the fracture (water-wet condition). These results encouraged us to develop a surfactant for Bakken shale to enhance waterflooding performance.

This paper presents a study of extensive experimental work done on Bakken shale reservoir core samples and crude oil with synthetic formation brine. The objective of this paper is to study the potential of surfactants to improve waterflooding performance in the Bakken shale formation by altering rock wettability. A series of experimental procedures were applied to test different surfactant capabilities with formation brine to alter Bakken rock wettability and improve recovery factors from spontaneous imbibition.

Pre-Screening Compatibility Test

In this test, synthetic 15%, and 30% brine solutions were used. The 30% brine represents in situ formation brine and 15% brine is used to represent the diluted formation water after waterflooding. Ten surfactants were tested in this screening step to identify the potential surfactants for later experiments. The recipe for synthetic brines is presented in Table 1.

After vigorous mixing for the synthetic brines and surfactants, the test tubes were set aside, and allowed to sit. All of the test tubes were placed in an oven held at 190°F. The clarity of each tube was monitored, and notes were taken of the appearance of each solution after sitting static for one week at 190°F.

Several developmental and commercial available products were tested (Figure 1). One of the formulas, (Stim aid A) surfactant, showed no precipitation in 15% or 30% brine using 0.1 wt.% and 0.2 wt.% concentrations at 190°F after one week. Since shale Bakken shale formation has ultra low permeability, so surfactants that show precipitation are not selected to not cause any formation damage even in the microscale. Surfactant with no precipitations means the surfactant is well compatible with the water and shale. Therefore, this study presents the results of this promising formula only.

TABLE 1 SYNTHETIC BAKKEN SHALE BRINE COMPOSITION

COMPONENT	15% SYNTHETIC BRINE	30% SYNTHETIC BRINE
	MG/L	
NACL	112,500	225,000
CACL2*2H2O	15,000	30,000
KCL	7,500	15,000
MGCL2*6H20	32,000	64,000

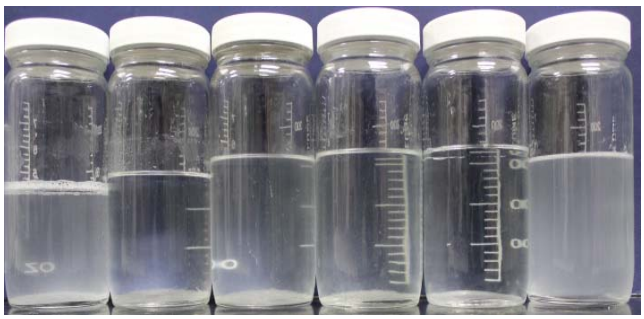

FIGURE 1. BRINE COMPATIBILITY TEST RESULTS FOR DIFFERENT SURFACTANTS AFTER ONE WEEK IN 15% AND 30% BRINES.

Surface Tension Measurements

A Kruss K100 unit was used to measure the surface

tension of the (Stim aid A) surfactant solutions with various concentrations from 0.05 wt.% to 0.4 wt.% in deionized water, and 15% brine at room temperature. Plate geometry was selected to do a static measurement. The calculation involved is shown in Figure 2.

Figure 3 shows the surface tension of different (Stim aid A) surfactant solutions from 0.05 wt.% to 0.4 wt.% in deionized water and 15% Brine. All solutions show relatively the same low surface tension, around 27 dynes/cm, because the critical micelle concentration of the (Stim aid A) surfactant is well below 0.05 wt.%. It also shows that the surface tension value of the (Stim aid A) surfactant solution is not affected by brine concentration.

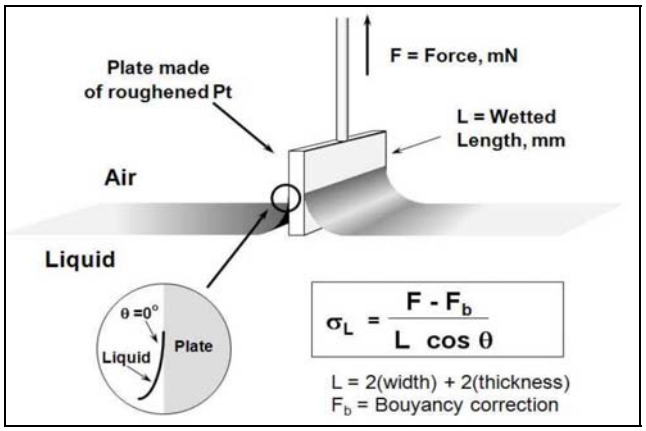

FIGURE 2. SURFACE TENSION CALCULATION FROM PLATE GEOMETRY MEASUREMENT IN KRUSS K100.

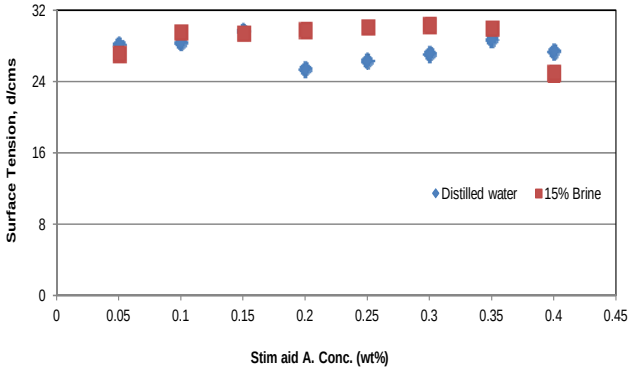

FIGURE 3. STIM AID A. SURFACE TENSION IN DIFFERENT SOLUTIONS.

Interfacial Tension Measurement

Interfacial Tension (IFT) measurements were performed using a spinning drop tensiometer (Figure 4). In this technique, a small oil drop (micro liters) is placed via a syringe inside a glass capillary tube that contains the surfactant solution to be evaluated. The heater is adjusted in the instrument to bring it up to the testing temperature (in this case 185°F). Then, the tube is spun at a very high speed (e.g. 5,000 rpm). This makes the spherical oil drop become a distorted "sausage shape." The IFT may be calculated based upon the shape of the oil drop (β), the angular velocity of rotation(ω), and the difference in the density between the oil and the aqueous surfactant solution (ϱ2-ϱ1), as shown in the following equation (Eq. 1), when the ratio of length to diameter of the oil drip is L/D ≥ 4.

$$IFT = \frac{(\rho_2 - \rho_1)\omega^2 D^2}{\beta^2} \quad (1)$$

From spinning drop measurements, the IFT of 0.1 wt.% (Stim aid A) surfactant in a 2% KCl brine was measured as 0.3 dyne/cm with Bakken crude oil drop.

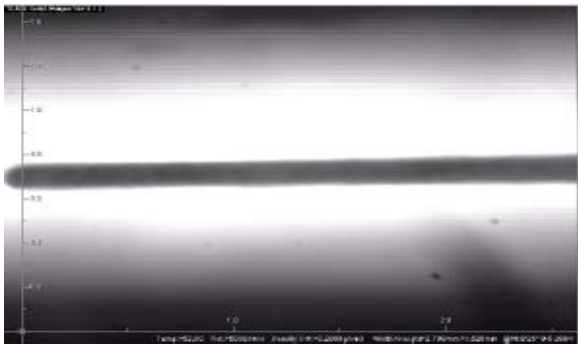

FIGURE 4. MAGNIFIED PHOTO OF AN OIL DROP BEING EVALUATED IN THE IFT MEASUREMENT.

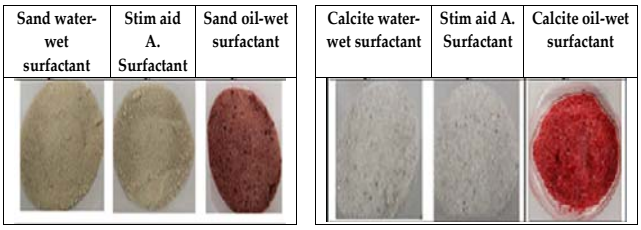

FIGURE 5. WETTABILITY RESULTS IN 15% SYNTHETIC BRINE WITH 40/60 WHITE SAND (LEFT) AND CALCITE (RIGHT).

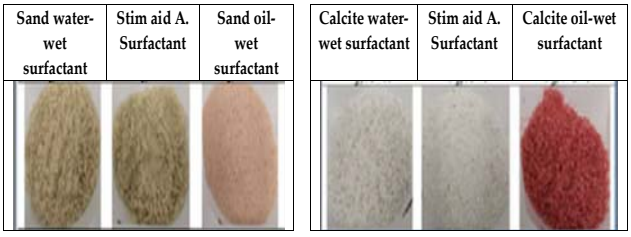

FIGURE 6. WETTABILITY RESULTS IN 30% SYNTHETIC BRINE WITH 40/60 WHITE SAND (LEFT) AND CALCITE (RIGHT).

Visual Assessment of Wettability

Visual wetting preference was assessed on disaggregated sand and marble. The (Stim aid A) surfactant was compared to a known water-wetting surfactant and an oil-wetting surfactant using 15% and 30% brine solutions. In order to show significant

colour contrast, high loading of surfactants were used in the study. Figures 5&6 show the resulting colour of 40/60 white sand and marble sand after they are exposed to the surfactant, followed by red dyed kerosene solution. Slightly yellow colour in white sand and white colour in marble sand mean the surfactants have strong water-wetting characteristics while red colour in both white sand and marble sand means surfactants tend to oil-wet the grain surfaces. The results indicated all test formulations have strong water wetting characteristics to both 40/60 white sand and marble sand.

Contact Angle Measurements

Use of the (Stim aid A) surfactant solutions could alter shale rock wettability, so we design our experiment to measure the contact angles of all samples used in the spontaneous imbibition experiments. Contact angles were measured using drop shape analysis with a drop size of 8 ml. contact. The method is to measure the angle of a sessile drop resting on a flat solid surface using a goniometer–microscope (Figure 7) equipped with a video camera and a suitable magnifying lens, interfaced to a computer with image-analysis software to determine the tangent value precisely on the captured image. A suitable cold light source and a sample stage whose elevation can be controlled to high precision are also required for the application of this technique. Formerly, the drop profile was photographed and the tangent of the sessile drop profile at the three-phase contact point was drawn onto the photo print to determine the value of the contact angle.

The contact angles were measured using fully oil saturated samples in only brine solutions (15% and 30%) as an initial condition. The same samples were then treated with 0.2 wt.% of the (Stim aid A) surfactant in 15% and 30% brine solutions for three hours when the final contact angles were measured.

The initial measured contact angles for the Bakken samples we tested were about 80º that implies intermediate wet characteristics, meaning that the Bakken rock surface had almost equal preference to oil and water (Figures 8&9). After only three hours of exposure with 0.2 wt.% of (Stim aid A) either in 15% or 30% brine solutions, the rock surface contact were lowered to about 20º that implies strongly water-wet characteristics (Figure 10). That change in rock surface wettability can enhance the release of oil from the rock as the surface rock preference to water increased and decreased to oil.

FIGURE 7. CONTACT ANGLE MEASUREMENT EQUIPMENT.

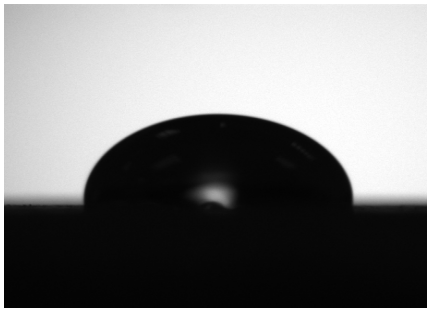

FIGURE 8. WATER DROPLET ON BAKKEN SHALE CORE SAMPLE BEFORE SURFACTANT TREATMENT.

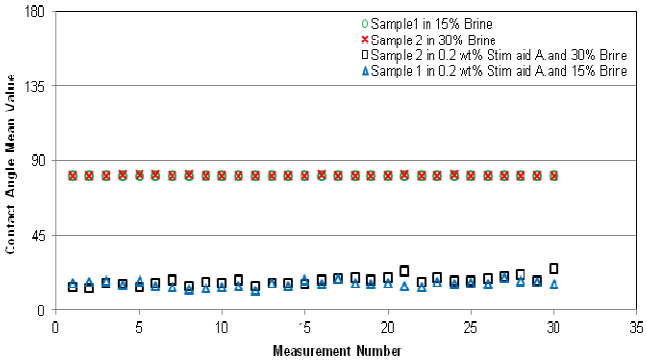

FIGURE 9. AVERAGE CONTACT ANGLES VALUES FOR BAKKEN SHALE CORES.

Spontaneous Imbibitions Experiment

Bakken reservoir cores (subject well/field) were from a depth of approximately 10,000 feet. The permeability to nitrogen was less than 0.05 md and porosity averaged 5.8%. To promote faster recovery, the plug samples were cut into smaller pieces. The helium pore volume was then determined for each piece.

To simulate the effect of preflood surfactant treatment on continued oil production, the test formation material (crude oil and surfactant solutions in the pore systems) were exposed to water imbibitions twice; the first time with surfactant for one week and the second time without surfactant for another week. In the first imbibitions experiment, the Bakken reservoir samples

were air dried, forced saturated/aged with Bakken crude oil, placed in Amott cells containing different surfactant solutions with different concentrations (0.1, 0.2 and 0.4 wt.%), and prepared with 15 and 30 wt.% brine solutions for one week. Spontaneous surfactant imbibition/oil production was recorded over time at 190°F.

In the second imbibition experiment, the same samples were air dried after the first imbibition with surfactant solutions and forced saturated/aged with Bakken crude oil. Then, the samples were placed again into the Amott cell with brine only (15% and 30% Brines), with no surfactant. Spontaneous water imbibition/oil production was recorded over time at 190°F. The average properties of the samples used in this study is presented in Table 2. The photograph in Figure 10 shows an Amott cell with Bakken core samples in different brine solutions. In spontaneous imbibition tests, the specific gravity of Bakken crude oil tested was 0.815 (42°API). The oil is quite light, making it favourable for use in the surfactant recovery process.

TABLE 2. BAKKEN SHALE SAMPLES PROPERTIES.

	Avg. bulk density (g/cc)	Avg. Porosity (%)	Solution of Imbibition
Set 1	2.74	4.93	15% Brine
Set 2	2.75	5.67	30% Brine
Set 3	2.74	6.11	15% Brine -previously treated with 0.1 wt% Stim aid A.
Set 4	2.76	5.63	15% Brine -previously treated with 0.2 wt% Stim aid A.
Set 5	2.75	6.23	30% Brine -previously treated with 0.1 wt% Stim aid A.
Set 6	2.75	6.40	30% Brine -previously treated with 0.2 wt% Stim aid A.

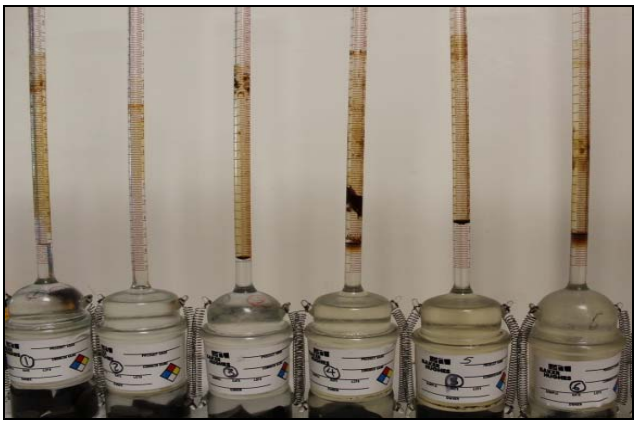

FIGURE 10. SHALE CORES AFTER 24 HOURS SOAKING IN THE DIFFERENT BRINE SOLUTIONS.

Figures 11 and 12 indicate additional oil production from cores pre-treated with 0.1 and 0.2 wt.% (Stim aid A.) surfactant in 15% and 30% brines (30-32%). The higher recovery was attributed to surfactant adsorption on the rock surface, altering the wetting preference during the pre-treatment of surfactant as supported by the contact angles and visual wettability experiments results.

In this paper, we presented the results using 0.2 wt.% surfactant concentration. Other concentrations were used elsewhere as discussed in the introduction. Higher concentrations were tested. The results showed higher adsorption (data unpublished) and it should be less economical. This study showed that 0.2 wt.% surfactant concentration worked. Considering other factors like adsorption, 0.2 wt.% of (Stim aid A.) surfactant is recommended in the preflood fluid to waterflooding in the Bakken shale.

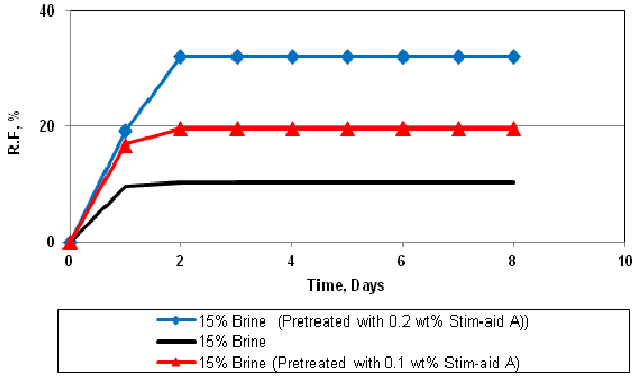

FIGURE 11. OIL RECOVERIES FROM BAKKEN SHALE CORES IN 15% BRINE.

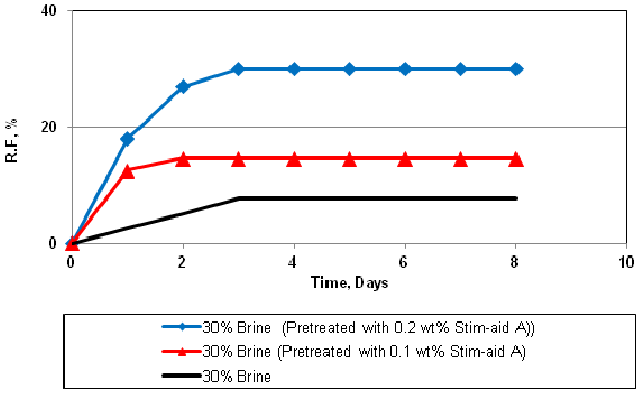

FIGURE 12. OIL RECOVERIES FROM BAKKEN SHALE CORES IN 30% BRINE.

Conclusions and Recommendations

- The Stim aid A. surfactant was fully compatible with formation brine and crude oil.
- Oil recovery was enhanced by wettability alteration when 0.2 wt.% of the (Stim aid A.) surfactant was used either with 15% or 30% synthetic formation brine solutions.
- It is recommended that 0.2 wt.% of (Stim aid A.) surfactant be used in the preflood fluid to waterflooding in the Bakken shale.

ACKNOWLEDGMENTS

The authors would like to acknowledge the generous support we received from Baker Hughes Company who provided us with the surfactants to complete this work.

REFERENCES

Fakcharoenphol, P., Charoenwongsa, S., Kazemi, H., & Wu, Y. S. (2012, January). The Effect of Water-Induced Stress to Enhance Hydrocarbon Recovery in Shale Reservoirs. In SPE Annual Technical Conference and Exhibition. Society of Petroleum Engineers.

Ferno, M. A., Haugen, A., & Graue, A. (2012, January). Surfactant Prefloods for Integrated EOR in Fractured Oil-Wet Carbonate Reservoirs. In SPE Annual Technical Conference and Exhibition. Society of Petroleum Engineers.

Goo, Q., Ji, L., Rajabov, V., Friedheim, J. E., Portella, C., & Wu, R. (2012, January). Shale gas drilling experience and lessons learned from Eagle Ford. In SPE Americas Unconventional Resources Conference. Society of Petroleum Engineers.

Killen J. C., and Biglarbigi K. Sep-2012. Oil Shale Research in the United States- Profiles of Oil Shale Research and Development Activities in Universities: National Laboratories, and Public Agencies. U.S. Department of Energy, Office of Petroleum Reserves, and Office of Naval Petroleum and Oil Shale Reserves. http://www.unconventionalfuels.org/publications/reports/Research_Project_Profiles_Book2011.pdf (accessed 20 Mar 2013).

Paktinat, J., Pinkhouse, J. A., Johnson, N., Williams, C., Lash, G. G., Penny, G. S., & Goff, D. A. (2006). Case study: Optimizing hydraulic fracturing performance in northeastern United States fractured shale formations. Paper SPE, 104306.

Wang, D., Butler, R., Liu, H., Liu, H., Ahmed, S., & Ahmed, S. (2011, January). Surfactant Formulation Study For Bakken Shale Imbibition. In SPE Annual Technical Conference and Exhibition. Society of Petroleum Engineers.

Xu, L., & Fu, Q. (2012, January). Ensuring Better Well Stimulation in Unconventional Oil and Gas Formations by Optimizing Surfactant Additives. In SPE Western Regional Meeting. Society of Petroleum Engineers.

Xu, L., & Fu, Q. (2012, January). Proper Selection of Surfactant Additive Ensures Better Well Stimulation in Unconventional Oil and Gas Formations. In SPE Middle East Unconventional Gas Conference and Exhibition. Society of Petroleum Engineers.